Energy 286 (2024) 129590

Contents lists available at ScienceDirect

Energy

journal homepage: www.elsevier.com/locate/energy

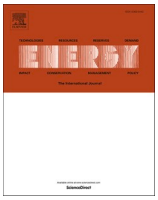

Hybrid modeling for the multi-criteria decision making of energy systems: An application for geothermal district heating system

Asli Ergenekon Arslan [a], Oguz Arslan [b,*], Mustafa Serdar Genc [c,d]

[a] Quality Control in Manufacturing Programme, Vocational School, Bilecik Seyh Edebali University, Bilecik, Turkey
[b] Mechanical Engineering Department, Engineering Faculty, Bilecik Seyh Edebali University, Bilecik, Turkey
[c] Energy Systems Engineering Department, Engineering Faculty, Erciyes University, Kayseri, Turkey
[d] Energy Conversion Research and Application Center, Erciyes University, Melikgazi, Turkey

ARTICLE INFO

Handling Editor: X Zhao

Keywords:
Artificial neural network
Analytic hierarchic process
Efficiency analysis
Geothermal district heating

ABSTRACT

The efficiency analysis technique with output satisficing (EATWOS) is a successful tool for determining the most efficient design for energy systems. Since EATWOS is rationally based on the maximal output throughout the minimal inputs, the weights of input and output values considerably affect the analysis results. Therefore, the impact ratio of each input and output term should be sensitively determined. In this study, the artificial neural network (ANN) modeling was used to determine the weights of the input values due to the quantitative effects of these values, whereas the analytical hierarchic process (AHP) was used for the output values due to qualitative effects. A new hybrid method was formed, embedding the ANN and AHP results into EATWOS. The new hybrid model was then applied to a sample geothermal district heating system for optimization. In this aim, 148 designs were formed throughout the different inlet parameters and evaluated by exergoeconomic and exergoenvironmental analysis to conduct the outputs. For the optimum case, the exergy efficiency was calculated as 20.25 %, whereas the SI was determined as 1.25, with the highest score. $1/r$ and $1/r_b$ were determined as 0.002337 and 0.001677, respectively. The NPV value was determined as 4.44 million $.

1. Introduction

Due to environmental concerns and experienced global crisis, the effective and efficient use of energy sources has become prominent. Therefore, it is vital to obtain maximal benefits from the energy systems through the minimal consumption of energy sources. In geothermal energy systems, the heat energy is supplied by the geothermal fluid. In that respect, geothermal energy is limited due to the reservoir capacities, although it is a renewable energy source. Therefore, it should be used efficiently for a sustainable future and geothermal resources [1–3]. It is the best practice to determine the most efficient systems for crowning with success. The multi-criteria decision-making (MCDM) analysis technique is a valuable tool for optimizing energy systems in this way.

Many studies about MCDM were conducted successfully for the energy systems in the literature. Roy [4] investigated the best performance of the biomass-based hybrid energy system involving a gasifier, fuel cell, gas turbine and Stirling engine. They used Vlsekriterijumska Optimizacija Kompromisno Resenje (VIKOR) technique in this aim. Toopshekan et al. [5] conducted a new approach for the optimization of a hybrid energy system involving a diesel generator, natural gas boiler, photovoltaic (PV), wind turbines (WT), and a battery system. In the study, the improved technique for order preference by similarity to an ideal solution (TOPSIS) weighted by the United Nations (UN) sustainable development goals method was used for the optimization. Li et al. [6] optimized a hybrid renewable energy system for rural areas, considering the PV, WT, hydropower, solar collectors and biogas systems. They used a combination weighting method, including criteria importance through inter-criteria correlation (CRITIC) and analytic hierarchy process (AHP) to determine the best decision for the hybrid system. Han et al. [7] investigated building performance optimization using MCDM. They used AHP to optimize the building energy performance along with the building structure. Ridha et al. [8] investigated the multi-objective optimization of standalone PV systems. They conducted that it was required to determine the best solution through MCDM techniques such as TOPSIS, AHP, decision-making trial and evaluation laboratory model (DEMATEL), weighted aggregated sum product assessment (WASPAS), preference ranking organization method for enrichment evaluations (PROMETHEE), and combined

* Corresponding author.
E-mail address: oguz.arslan@bilecik.edu.tr (O. Arslan).

https://doi.org/10.1016/j.energy.2023.129590
Received 8 August 2023; Received in revised form 25 October 2023; Accepted 4 November 2023
Available online 8 November 2023

distance-based assessment (CODAS). Li et al. [9] developed a decision-making framework to determine the optimal scheme of a biomass gasification-based cogeneration system. The study used the linear programming technique for multidimensional analysis of preference (LINMAP) for decision-making. Hai et al. [10] investigated the performance optimization of a solar heat pump system. In the study, they optimized the system by AHP after they solved the system parameters through the artificial neural network (ANN) tool. Arslan and Arslan [11] determined the optimal solution of a thermal energy storage (TES) integrated geothermal district heating system (GDHS) through MCDM analysis. They used the efficiency analysis technique with output satisficing (EATWOS) tool in the optimization stage. In another study, Arslan et al. [12] investigated TES-driven heat pump (HP) integrated GDHS. They used EATWOS to determine the optimal solution of the GHDS's optimal working parameters.

As seen from the mentioned literature, MCDM is a valuable tool to determine the optimal or the best solution for energy systems. However, it is still possible to boost the solutions of the MCDM technique. The hybrid models, obtained by integrating different analysis techniques, become prominent in this aim. Zhao et al. [13] investigated the performance evaluation index of combined cooling, heating and power from the economic, environmental and energy points of view. The study proposed a new hybrid MCDM model based on the integrated subjective and objective weighting obtained by the anti-entropy weight (AEW) method and the grey decision-making trial and evaluation laboratory (grey-DEMATEL). The obtained weights were evaluated by the TOPSIS combined with difference and quotient grey relation analysis (DQGRA) to perform the efficiency of the handled energy system. Bac et al. [14] comprehensively evaluated the heating, ventilating and air-conditioning (HVAC) system by a hybrid MCDM. They determined the weights using the stepwise weight assessment ratio analysis (SWARA) to perform the weighted additive sum product assessment (WASPAS) for the comparison of the handled HVAC systems. Manirambona et al. [15] evaluated power technologies' economic, social, technical and environmental dimensions through the hybrid MCDM technique. They combined AHP and TOPSIS to evaluate 17 energy indicators with this aim. Arslan et al. [16] investigated the optimal integrated geothermal energy system, including power generation, residence heating and greenhouse heating. The AHP-TOPSIS hybrid method was developed to make a decision on the best integration considering the different essential targets. Usman et al. [17] investigated the building-level performance indicators for renewable energy integrated energy supply and HVAC systems. They determined the best HVAC option by using the CRITIC-TOPSIS hybrid MCDM tool. Yang et al. [18] evaluated renewable energy heating systems by a novel multilevel decision-making approach. In this aim, they offered a new hybrid MCDM method, including CRITIC and fuzzy analytic hierarchy process (FAHP). Oner and Khalilpour [19] evaluated different hydrogen carriers to determine the best solution. In this aim, they evaluated nine criteria through hybrid models of AHP-TOPSIS and AHP-VIKOR. Abdel-Basset et al. [20] evaluated the sustainable locations for PV farms using hybrid MCDM analysis. They hybridized DEMATEL and VIKOR tools with this aim. Abdel-Basset et al. [21], in another study, investigated the sustainability of bioenergy production technologies. They hybridized DEMATEL and the evaluation based on distance from average solution (EDAS) methods to determine the best solution amongst the seven alternatives. Saraswat and Digalwar [22] investigated the alternative energy scenarios for sustainable development in India. They integrated Shannon's entropy method (SEM) into AHP. They used SEM to determine the weights of decision units. Elkadeem et al. [23] investigated the sustainable location and optimization of the hybrid renewable energy system, including PV and WT. They used a hybrid MCDM model for the best solution, including the best-worst method (BWM) and TOPSIS (or VIKOR). The geographical information system (GIS) based BWM was used to determine the weightings of performance indicators. All the studies conducted in the literature show that the hybrid MCDM technique yields successful results on the best solution for energy systems.

However, in the designing problems of the energy systems, including numerical thermodynamic parameters such as pressure and temperature, the weightings of these parameters are much more important for a sensible decision since the outputs are directly affected by the variation of those. Therefore, the effects of these parameters should be properly determined. ANN models can sensitively measure the degree of influence since these models yield agreeable results with successful high scores [24–26]. This study proposed a new hybrid MCDM method to determine the best design for a new GDHS involving a domestic TES-driven HP system. In this aim, 148 designs were conducted by the analytic method considering different thermodynamic parameters. Temperature scales, pressure scales related to temperature, and different refrigerants were handled as the input parameters. The output parameters were handled as the exergy efficiency, exergoeconomic and exergoenvironmental factors to measure the exergetic, environmental and economic relations.

Additionally, the net present value (NPV) and sustainability index (SI) were taken into account to measure the investment grade and the sustainable use of the sources. As the first step, an ANN model was established to determine the effects of the input parameters on the system's outputs. As the second step, AHP was performed for the output parameters to determine significance levels considering the expert views since the output parameters qualitatively affect the optimal solution. Finally, the hybrid MCDM model was established by integrating the obtained weighting scores into the efficiency analysis technique with output satisficing (EATWOS).

2. Methodology

A new hybrid method was formed, embedding the ANN and AHP results into EATWOS. Due to quantitative effects, the ANN modeling was used to determine the weights of the input values. The AHP was used for the out values due to qualitative effects. The flow chart of the modeling is given in Fig. 1.

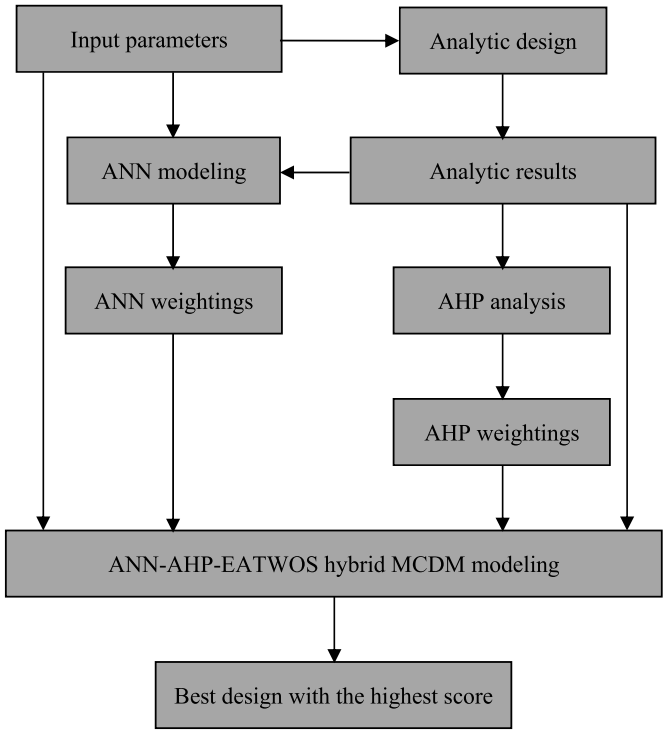

Fig. 1. Flow chart of ANN-AHP-EATWOS hybrid modeling.

2.1. ANN modelling

ANN can be successfully applied for optimizing energy systems involving normal varying parameters. However, the optimization process is very complicated for the systems involving irregular variations, although the ANN is sufficient to estimate results. Nevertheless, the ANN tool can be used to determine input variables' effects on the systems' outputs.

In an ANN, weight values drive the network to reach knowledge through building relationships between the inputs and outputs. A learning algorithm is used to obtain these relationships. In this study, the feed-forward back-propagation training algorithm, which is most widely used, was handled in the multi-layer neural network (MLNN) architecture. In this study, the Levenberg-Marguardt (LM) algorithm was selected as the training algorithm since it has successful scores for energy design problems [27–29]. The structure of the ANN is given in Fig. 2. According to Fig. 2, x_i defines the inlet parameters. $w_{i,j}$ defines the weighting multipliers for the ith inlet parameter and jth outlet. b_j is the bias value for the jth outlet parameter.

All the temperature values that describe the design points of the handled systems were selected as input neurons. The working fluids were introduced to analysis through their specific heat (Cp) values since they directly affect the design calculations. As seen in Fig. 2, a single-layered (without hidden layer) ANN structure was trained since it was aimed to obtain the weights of the ANN structure. By doing so, the effect of the bias in multi-criteria analysis could be prevented. In the analysis, the inputs and outputs are normalized in the range of 0.3 and 0.7 to scale all parameters in the equivalent degree. In this range, the effects of the absorbing and identity elements were also prevented. The Levenberg-Marguardt (LM) algorithm was used as the training along with the linear transfer function (Purelin) to see the effects of inputs on the outputs. The Purelin function for the inputs in a number of k is given as:

$$y_j = \sum_{i=1}^{k} w_{i,j} x_i + b_j \tag{1}$$

Seventy percent of the formed designs were included in the ANN for the training stage; the remaining part was used to test the network. The accuracy of the network was separately measured for the training and testing stages by the coefficient of multiple determinations (R^2). In terms of the predicted output (y_{ANN}), actual output (y_{actual}) and the mean actual output ($\overline{y}_{actual}$), R^2 is given for the designs in a number of m:

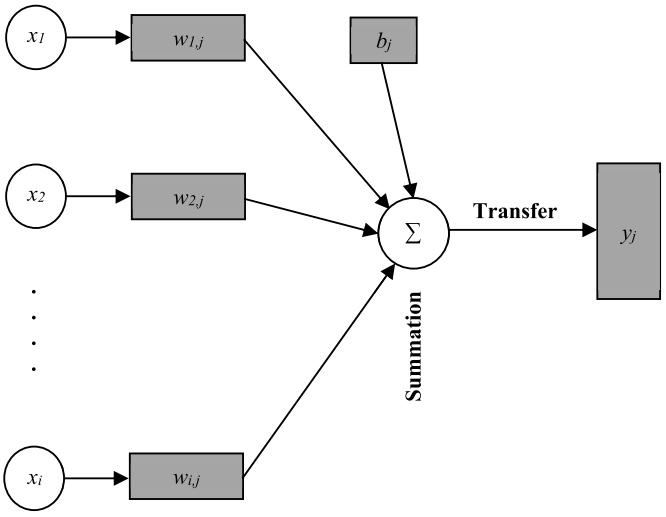

Fig. 2. The structure of the used ANN.

$$R^2 = 1 - \frac{\sum_{i=1}^{m} \left(y_{ANN} - y_{actual}\right)^2}{\sum_{i=1}^{m} \left(y_{actual} - \overline{y}_{actual}\right)^2} \tag{2}$$

when the ANN results are satisfied, the weightings (δ) of the input parameter for the jth output are obtained by:

$$\mathbf{W}_{ANN} = \begin{bmatrix} \delta_{1j} = \dfrac{w_{1j}}{\sum_{k=1}^{n} w_{kj}} \\ \vdots \\ \delta_{kj} = \dfrac{w_{kj}}{\sum_{k=1}^{n} w_{kj}} \end{bmatrix} \tag{3}$$

2.2. AHP analysis

AHP, conducted by Myers and Alpert [30], includes a decision hierarchy in which the decision points are compared with each other. So, the AHP can determine the importance degree of the output parameters in a weighting matrix (the priority vector). The formation of this matrix spiritedly is based on expert views, which can be easily determined by a comparing scale given in Table 1 [31].

According to this scale, a comparison matrix is formed for the output parameters (decision points) in a number n of the energy problem. Taking the relationship of $a_{ji} = \frac{1}{a_{ij}}$ between the matrix elements, the comparison matrix is given by Ref. [32]:

$$\mathbf{A} = \begin{bmatrix} 1 & \cdots & a_{1n} \\ \vdots & \ddots & \vdots \\ a_{n1} & \cdots & 1 \end{bmatrix} \tag{4}$$

where a_i is the importance scale of the ith criteria in comparison to the jth criteria. For the next step, $\mathbf{A}$ is normalized using the formulation of $b_{ij} = \frac{a_{ij}}{\sum_{i=1}^{n} a_{ij}}$ to give the significance matrix $\mathbf{B}$:

$$\mathbf{B} = \begin{bmatrix} b_{11} & \cdots & b_{1n} \\ \vdots & \ddots & \vdots \\ b_{n1} & \cdots & b_{nn} \end{bmatrix} \tag{5}$$

Finally, the priority vector ($\mathbf{W}_{AHP}$) is generated to determine the weightings of the outputs as:

$$\mathbf{W}_{AHP} = \begin{bmatrix} v_1 \\ \vdots \\ v_n \end{bmatrix} \tag{6}$$

where v_n is calculated with the following equation;

$$v_n = \frac{\sum_{j=1}^{n} b_{ij}}{n} \tag{7}$$

in AHP, it is necessary to verify expert views. So, the consistency of the determined weights (CR) should be less than 0.10 for an acceptable

Table 1
Importance scale.

Scale	Value Definitions
1	The equal importance of both factors
3	The first factor is more important than the second factor
5	The first factor is much more important than the second factor
7	The fact that the first factor has extreme importance compared to the second factor
9	The fact that the first factor has absolute superiority than the second factor
2,4,6,8	Intermediate values

decision. In terms of the consistency indicator (*CI*) and random indicators (*RI*), *CR* is given as:

$$CR = \frac{CI}{RI} = \frac{\frac{\sum_{j=1}^{n} \frac{c_j}{v_i}}{n} - n}{(n-1)RI} \tag{8}$$

where c_i is obtained from:

$$\mathbf{C} = \begin{bmatrix} c_1 \\ \vdots \\ c_n \end{bmatrix} = \begin{bmatrix} 1 & \cdots & a_{1n} \\ \vdots & \ddots & \vdots \\ a_{n1} & \cdots & 1 \end{bmatrix} \bullet \begin{bmatrix} v_1 \\ \vdots \\ v_n \end{bmatrix} \tag{9}$$

2.3. ANN-AHP-EATWOS hybrid analysis

Efficiency Analysis Technique with Output Satisficing (EATWOS) is a successful technique depending on the satisfied results for energy problems [11,12]. EATWOS analysis compares the conducted designs, considering the input and output values to measure the efficiencies of the designs. EATWOS aims to give the highest efficiency with minimum inputs. The efficiency of EATWOS for the ith design is given as [33]:

$$E_i = \frac{\sum_{j=1}^{J} v_j \bullet op_{ij}}{\sum_{k=1}^{K} \delta_k \bullet ip_{ik}} \tag{10}$$

where δ_k and v_j are input and output parameter weights, respectively. ip_{ik} and op_{ik} are the distance matrices for the input and output values, respectively, and are given by:

$$ip_{ik} = 1 + s_{ik} - s_k^* \tag{11}$$

$$op_{ij} = 1 + r_{ij} - r_j^* \tag{12}$$

where s_{ik}, r_{ij}, s_k^* and r_j^* are respectively normalized input, normalized output, maximum normalized input and maximum normalized output values, and are given as follows:

$$s_{ik} = \frac{x_{ik}}{\sqrt{\sum_{i=1}^{K} x_{ik}^2}} \tag{13}$$

$$r_{ij} = \frac{y_{ij}}{\sqrt{\sum_{i=1}^{I} y_{ij}^2}} \tag{14}$$

$$s_k^* = \min_i \{s_k\} \tag{15}$$

$$r_j^* = \max_i \{r_j\} \tag{16}$$

The input and output values are multiplied by a weight factor to perform the variation in terms of the importance level of each parameter. Since these levels are critical to obtain sensitive results, they should be determined carefully. In this aim, ANN is a valuable tool to determine the weightings depending on the quantitative effects of the variation of the input parameters, whereas the AHP is a valuable tool to determine the weightings depending on the qualitative effects of the variation of the output parameters. So, the efficiency of the ANN-AHP-EATWOS hybrid model of the *i*th design with inlet parameters in a number of *k* is given by:

$$E_{hybrid,i} = \sum_{j=1}^{n} \frac{[op_j] \bullet [v_j]_{AHP}}{[ip_1 \quad \cdots \quad ip_k] \bullet \begin{bmatrix} \delta_{1j} \\ \vdots \\ \delta_{kj} \end{bmatrix}_{ANN}} \tag{17}$$

where *j* indicates the output parameter obtained by the thermodynamic analysis of the energy system. The used weights of ANN characterize the degree of influence of the input parameters more accurately in the EATWOS, whereas the used weights of AHP characterize the degree of influence of the output parameters more accurately in the EATWOS. Therefore, the obtained results by the hybridized ANN-AHP-EATWOS model would be more agreeable for the optimization problems of the energy systems.

3. Case study

A new GDHS, designed considering the Simav geothermal resources, was selected as the optimization problem in the study. The system is formed of three subsystems, namely the heat center (C), substation (S) and heating circuit (HC). The schematic of GDHS is given in Fig. 3.

According to Fig. 3, the geothermal fluid is transmitted to C by the pump (P1) along the geothermal transmission line (GTL) with a 4250 m length (points 1–2). In C, the heat of the geothermal fluid (points 1–2) is transferred to the fluid (water) of district heating (points 4–9) by a plate-type heat exchanger (HEx). The heated district water is later transmitted to the S along the district transmission line (DTL) with a 4000 m length (points 4–5) by the pump (P2). In S, the heat of the district water is stored in the TES (or evaporator) unit (points 5–8) to be transferred to the refrigerant of the vapour-compressed HP system (points a-d). Later, the heated refrigerant is compressed to the working pressure (points a-b) by the compressor (Comp) to be sent to the condenser (Con). In Con, the heat of the refrigerant is transferred to the fluid (water) of HC (points b-c). In the expansion valve (EV), the refrigerant is expanded to TES pressure (points c-d), and the cycle is completed. The heated HC fluid is finally transferred to the aluminum panel radiator system (Rad) by the circulation pump (P3) to heat the residences (points 6–7).

According to the designed system given in Figs. 2 and 148 designs were formed considering different thermodynamic working parameters, phase change materials (PCM) and working fluids. In this aim, 3 different PCMs in the TES system and 3 different working fluids in the HP system were performed. The PCMs were selected considering the handled parametric temperature values of the system at the designing stage. The working fluids were selected considering the thermophysical properties such as melting temperature (T_m), latent heat capacity and corrosive effects, as well as the environmental properties such as ozone depletion rate (ODP) and global warming potential (GWP). In this regard, R600a as the dry type, R290 as the wet type and R1234ze as the isentropic type were used in the analysis, whereas organic materials (RT55, RT60 and RT70HC) were used. The properties of the used PCM and working fluids are given in Table 2.

In the optimization aim of the new hybrid model, the working temperatures of the system were selected as the input parameters (x_{ij}). The pressure values were determined according to the handled temperature

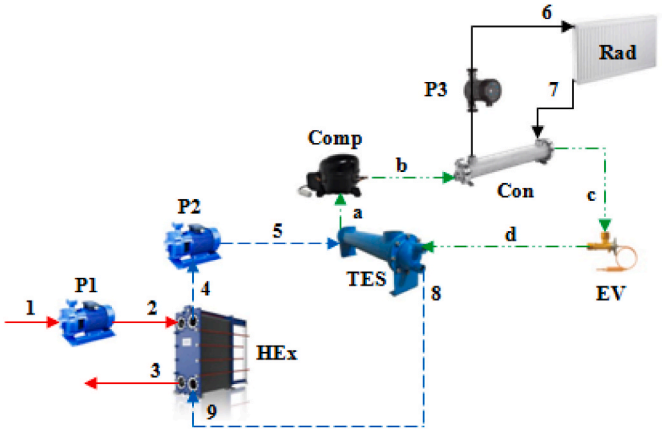

Fig. 3. Schematic of TES-driven HP system integrated GDHS.

Table 2
Properties of PCM and working fluid used in the system [34–37].

Properties	R600a	R290	R1234ze	RT55	RT60	RT70HC
Boiling Point (°C)	−11.75	−42.11	−18.95	–	–	–
Critical Temperature (°C)	134.66	96.74	109.37	–	–	–
Critical Pressure (MPa)	3.63	4.25	3.64	–	–	–
Density, ρ (kg/m^3)	508.69[a]	436.66[a]	1049.60[a]			
Liquid	–	–	–	770	770	770
Solid	–	–	–	880	880	880
Volumetric expansion, β	–	–	–	1.14	1.14	1.14
Latent heat capacity (kJ/kg)	–	–	–	140	130	230
Conductive heat transfer coefficient, k (W/mK)	–	–	–	0.2	0.2	0.2
Dynamic viscosity, μ (Ns/m^2)	–	–	–	0.01	0.01	0.01
Specific heat, C_p (kJ/kg K)	2.67[a]	3.23[a]	1.53[a]	2	2	2
Melting temperature, T_m (°C)	–	–	–	55	60	70
ODP	0	0	0	–	–	–
GWP	3	3	1	–	–	–

[a] values at 56, C, ODP: ozone depletion rate, GWP: global warming potential.

values through RefProp [34] since they were necessary for the required power consumption. In the calculations, the efficiencies (η) of the pumps and compressor were assumed to be 80 %, whereas the efficiencies of the heat exchangers were assumed to be 98 %. Also, the minimum temperature differences between the cold and hot streams were kept at 5 °C for the liquid phases and 10 °C for the gas phases [12]. Under these assumptions, the used parameters in the analysis are given in Table 3.

3.1. Thermodynamic analysis

The mass, energy, and exergy balances of the *k*th component under steady-state conditions are given by:

$$\sum(\dot{m}_i)_k - \sum(\dot{m}_o)_k = 0 \tag{18}$$

$$\dot{Q}_k - \dot{W}_k + \sum(\dot{m}_i h_i)_k - \sum(\dot{m}_o h_o)_k = 0 \tag{19}$$

$$\left(1 - \frac{T_0}{T}\right)\dot{Q}_k - \dot{W}_k - \sum(\dot{m}_i \psi_i)_k - \sum(\dot{m}_o \psi_o)_k - \dot{E}x_{d,k} = 0 \tag{20}$$

where $\dot{Q}$, $\dot{W}$, and $\dot{E}x_{d,k}$ are the heat rate, work rate, and exergy destruction, respectively. The specific exergy of a flow (ψ) at a particular state is given by:

$$\psi = (h - h_0) - T_0(s - s_0) \tag{21}$$

where h and s indicate the enthalpy and entropy, respectively. The subscript "0" defines the reference conditions at 25 °C and 1 atm. The energy and exergy balances of the GDHS are given in Table 4.

3.2. Exergoeconomic and exergoenvironmental analysis

The exergoeconomic and the environmental impact balances of the *k*th component and jth stream-related are respectively given by Refs. [38,39]:

Table 3
The design parameters used in the analysis.

Design parameters		Value		
		R600a	R290	R1234ze
Input (x_{ij}) parameters	T_1 (°C)	95, 100, 110		
	T_2 (°C)	a		
	T_3 (°C)	a		
	T_4 (°C)	T_2 (°C)-5		
	T_5 (°C)	a		
	T_6 (°C)	45, 50, 55, 60		
	T_7 (°C)	T_6 - ΔT; ΔT = 10, 15, 20		
	T_8 (°C)	$T_m + \Delta T$; min ΔT = 5		
	T_9 (°C)	a		
	T_a (°C)	$T_m + \Delta T$; min ΔT = 10		
	T_b (°C)	a		
	T_c (°C)	T_7+ ΔT; min ΔT = 5		
	T_d (°C)	T_a - ΔT; min ΔT = 10		
	T_m (°C)	55, 60, 70		
P_a (kPa)		350.7–545.3	836.5–1401.3	513.9–787.7
P_b (kPa)		635.7–1087.5	1604.2–2586.8	923.4–1611.1
η_P (%)		80		
η_{Comp} (%)		80		
ηHEx - ηTES - ηCon (%)		98		

[a] calculated values via the thermodynamic analysis.

Table 4
Energy and exergy balance equations.

Components	Energy balance	Exergy balance
HEx	$\dot{Q}_{HEx} = (\dot{m}h_3 - \dot{m}h_2)\eta_{HEx} - (\dot{m}h_9 - \dot{m}h_4)$	$\dot{E}x_{HEx} = (\dot{m}\psi_2 - \dot{m}\psi_3) + (\dot{m}\psi_9 - \dot{m}\psi h_4) - \left(1 - \frac{T_0}{T_{ave}}\right)\dot{Q}_{HEx}$
TES	$\dot{Q}_{TES} = (\dot{m}h_8 - \dot{m}h_5) - (\dot{m}h_a - \dot{m}h_d)$	$\dot{E}x_{TES} = (\dot{m}\psi_5 - \dot{m}\psi_8) + (\dot{m}\psi_d - \dot{m}\psi_a) - \left(1 - \frac{T_0}{T_{ave}}\right)\dot{Q}_{TES}$
Con	$\dot{Q}_{Con} = (\dot{m}h_c - \dot{m}h_b)\eta_{Con} - (\dot{m}h_7 - \dot{m}h_6)$	$\dot{E}x_{TES} = (\dot{m}\psi_b - \dot{m}\psi_c) + (\dot{m}\psi_7 - \dot{m}\psi_6) - \left(1 - \frac{T_0}{T_{ave}}\right)\dot{Q}_{Con}$
Comp	$\dot{Q}_{Comp} = (\dot{m}h_b - \dot{m}h_a) - \dot{W}_{Comp}$	$\dot{E}x_{d,Comp} = (\dot{m}\psi_a - \dot{m}\psi_b) + \dot{W}_{Comp} - \left(1 - \frac{T_0}{T_{ave}}\right)\dot{Q}_{Comp}$
Read	$\dot{Q}_{useful} = \dot{m}h_7 - \dot{m}h_6$	$\dot{E}x_{d,Rad} = (\dot{m}\psi_6 - \dot{m}\psi_7) - \left(1 - \frac{T_0}{T_{ave}}\right)\dot{Q}_{useful}$
EV	$\dot{Q}_{Eva} = \dot{m}h_d - \dot{m}h_c$	$\dot{E}x_{d,Eva} = (\dot{m}\psi_c - \dot{m}\psi_d) - \left(1 - \frac{T_0}{T_{ave}}\right)\dot{Q}_{Eva}$
P1	$\dot{Q}_{P1} = (\dot{m}h_2 - \dot{m}h_1) - \dot{W}_{P1}$	$\dot{E}x_{d,P1} = (\dot{m}\psi_1 - \dot{m}\psi_2) + \dot{W}_{P1} - \left(1 - \frac{T_0}{T_{ave}}\right)\dot{Q}_{P1}$
P2	$\dot{Q}_{P2} = (\dot{m}h_5 - \dot{m}h_4) - \dot{W}_{P2}$	$\dot{E}x_{d,P2} = (\dot{m}\psi_4 - \dot{m}\psi_5) + \dot{W}_{P2} - \left(1 - \frac{T_0}{T_{ave}}\right)\dot{Q}_{P2}$
P3	$\dot{Q}_{P3} = (\dot{m}h_6 - \dot{m}h_7) - \dot{W}_{P3}$	$\dot{E}x_{d,P3} = (\dot{m}\psi_7 - \dot{m}\psi_6) + \dot{W}_{P3} - \left(1 - \frac{T_0}{T_{ave}}\right)\dot{Q}_{P3}$
Overall system		$\dot{E}x_{d,total} = \dot{E}x_{d,HEx} + \dot{E}x_{d,TES} + \dot{E}x_{d,Comp} + \dot{E}x_{d,Rad} + \dot{E}x_{d,Eva} + \dot{E}x_{d,P1} + \dot{E}x_{d,P2} + \dot{E}x_{d,P3}$

$$\sum c_{out}\dot{E}x_{out,k} + c_W\dot{W}_{W,k} = \sum c_{in}\dot{E}x_{in,k} + c_Q\dot{E}x_{Q,k} + \dot{Z}_k \quad (22)$$

$$c_F\dot{E}x_{F,k} + \dot{Z}_k = c_P\dot{E}x_{P,k} \quad (23)$$

$$\sum b_j\dot{E}x_j + \left(\dot{Y}_k^{CO} + \dot{Y}_k^{OM} + \dot{Y}_k^{D}\right) = \sum \dot{B}_{j,k,out} \quad (24)$$

where c is the unit cost of exergy flow. The subscripts *in, out, Q, W, F,* and P define the inlet, outlet, heat-related terms, work-related terms, fuel and product, respectively. b_j is the specific environmental impact. $\dot{Y}_k^{CO}$, $\dot{Y}_k^{OM}$, and $\dot{Y}_k^{D}$ are environmental impacts of the life cycle phases including construction, operation and maintenance, and disposal, respectively. $\dot{Z}$ indicates the investment cost rate of the kth component and is given by Ref. [39]:

$$\dot{Z}_k = \frac{Z_0\varphi}{N}\frac{i(1+i)^n}{(1+i)^n - 1} \quad (25)$$

in this study, φ was taken as 1.06, N was taken as 2683 h, n was assumed as 20 years, and inflation rate (i) was taken as 15.75 % [12,39]. Cost balances, environmental impact balances and auxiliary equations of the GDHS are given in Table 5.

3.3. Design criteria of the GDHS

At the designing stage, the required sizes of the used components were determined considering the parametric working conditions of the proposed GDHS. The required sizes were determined considering the peak heat demand of 4.5 kW [12]. Besides, all the losses, such as heat and pressure, were determined in the care of the required sizes. Therefore, the thermodynamic, economic and environmental relations could be built to determine decision points of designed system configurations.

Accordingly, an aluminum panel radiator (Rad) with a nominal height of 0.6 m was selected to supply the required peak heating demand in HC. The required Rad lengths were determined considering the production company's data for the different temperature scales [41].

In C, a plate-type heat exchanger with titanium coating (HEx) was handled as appropriate to the current status. Using this kind of heat exchanger also aims to prevent the corrosion effects of the geothermal fluid. The exchanger's efficiency was assumed to be 0.98 to cope with the worst cases. In terms of the required heat transfer area, the numbers of the plates are given by Refs. [42,43]:

$$n_{plate} = \frac{A_{HEx}}{A_{plate}} = \frac{\frac{0.98\dot{m}_2(h_2-h_3)}{U_{Hex}\left(\frac{(T_2-T_4)-(T_3-T_9)}{ln\left(\frac{T_2-T_4}{T_3-T_9}\right)}\right)}}{1.38} \quad (26)$$

in S, an HP system was used to boost the supplied heat. By doing so, it was aimed to increase the sustainability of geothermal resources. A TES system drove the HP system to prevent the wastage of energy of GDHS. The TES system was used as an evaporator in the form of a shell and tube-type heat exchanger. The tube side includes two kinds of pipes, namely heating and cooling pipes; therefore, it is available to operate simultaneously for both charging and discharging at the peak load demands. The shell side is filled with paraffin wax as the phase change material (PCM) [12]. The required pipe numbers ($_{pipe}$) and the related TES volume (V_{TES}) are given by:

$$n_{pipe,charging} = \frac{\dot{Q}_{design}}{U_{pipe,charging}A_{pipe,charging}\left(\left(\frac{T_5+T_8}{2}\right) - T_m\right)} \quad (27)$$

$$n_{pipe,discharging} = \frac{\dot{Q}_{design}}{U_{pipe,discharging}A_{pipe,discharging}\left(T_m - \left(\frac{T_a+T_d}{2}\right)\right)} \quad (28)$$

$$V_{TES} = \left(A_{pipe}\bullet\left(n_{pipe,charging} + n_{pipe,discharging}\right)\bullet H\right) + \left(\frac{86400\bullet\left(\dot{Q}_{design} + U_{shell}A_{TES}(T_{TES} - T_{ambinece})\right)}{Q_{TES}}\bullet\beta\right) \quad (29)$$

where $\dot{Q}_{design}$ is the heat demand for 12,500 residences (56,130 kW). A_{pipe} and T_m indicate the heat transfer area of the charging and discharging pipes and the melting temperature of PCM, respectively. H and β are the TES unit's height and PCM thermal expansion coefficient, respectively. U_{shell}, $U_{pipe,\ charging}$ and $U_{pipe,\ discharging}$ are the heat transfer coefficients of the shell side, charging tubes and discharging tubes. The condenser (Con) was handled as the shell and tube-type heat exchanger. It was assumed that the refrigerant was circulating on the tube side. The required heat transfer area of Con is given by:

$$A_{condenser} = \frac{\dot{Q}_{design}}{U_{Con}\left(\frac{(T_6-T_b)-(T_7-T_c)}{ln\left(\frac{T_6-T_b}{T_7-T_c}\right)}\right)F} \quad (30)$$

where ΔT_{lm} and F are the logarithmic mean temperature and correction factor, respectively [42,44]. The heat loss for transmission pipelines with a length of L is given by:

$$\dot{Q}_{loss,transmission} = \frac{2\pi L(T_i - T_o)}{R} \quad (31)$$

Table 5
Exergoeconomic cost balances, environmental impact balances and auxiliary equations [12,40].

Components	Cost balance	Balance equation	Auxiliary equation
HEx	$\dot{C}_2 + \dot{C}_9 + \dot{Z}_{HEx} = \dot{C}_3 + \dot{C}_4$	$\dot{B}_2 + \dot{B}_9 + Y_{HEx} = \dot{B}_3 + \dot{B}_4$	$c_2 = c_3$, $b_2 = b_3$ $c_8 = c_9$, $b_8 = b_9$
TES	$\dot{C}_5 + \dot{C}_d + \dot{Z}_{TES} = \dot{C}_a + \dot{C}_8$	$\dot{B}_5 + \dot{B}_d + Y_{TES} = \dot{B}_a + \dot{B}_8$	$c_5 = c_8$, $b_5 = b_8$
Con	$\dot{C}_b + \dot{C}_7 + \dot{Z}_{Con} = \dot{C}_c + \dot{C}_6$	$\dot{B}_b + \dot{B}_7 + Y_{Con} = \dot{B}_c + \dot{B}_6$	$c_b = c_c$, $b_b = b_c$
Comp	$\dot{C}_4 + \dot{C}_6 + \dot{C}_{W,P2} + \dot{Z}_{H-line} = \dot{C}_5 + \dot{C}_7$	$\dot{B}_5 + \dot{B}_{11} + \dot{B}_{W,P3} + \dot{Y}_{TES} = \dot{B}_6 + \dot{B}_8$	$c_6 = c_7$ $c_{W,P2} = 0.5\frac{\$}{MJ}$, $b_6 = b_7$ $b_{W,P2} = 7.5\frac{mPts}{MJ}$
Read	$\dot{C}_6 + \dot{Z}_{Rad} = \dot{C}_7$	$\dot{B}_6 + \dot{Y}_{Rad} = \dot{B}_7$	–
EV	$\dot{C}_c + \dot{Z}_{Eva} = \dot{C}_d + \dot{C}_{Q,Eva}$	$\dot{B}_c + \dot{Y}_{Eva} = \dot{B}_d + \dot{B}_{Q,Eva}$	$c_{Q,Eva} = 0.0511\frac{\$}{MJ}$, $b_{Q,Eva} = 5.4\frac{mPts}{MJ}$
P1	$\dot{C}_1 + \dot{C}_{W,P1} + \dot{Z}_{P1} = \dot{C}_2$	$\dot{B}_1 + \dot{B}_{W,P1} + \dot{Y}_{P1} = \dot{B}_2$	$c_1 = 0$ $c_{W,P1} = 0.5\frac{\$}{MJ}$, $b_1 = 0$ $b_{W,P1} = 7.5\frac{mPts}{MJ}$
P2	$\dot{C}_4 + \dot{C}_{W,P2} + \dot{Z}_{P2} = \dot{C}_5$	$\dot{B}_4 + \dot{B}_{W,P2} + \dot{Y}_{P2} = \dot{B}_5$	$c_{W,P2} = 0.5\frac{\$}{MJ}$, $b_{W,P2} = 7.5\frac{mPts}{MJ}$
P3	$\dot{C}_7 + \dot{C}_{W,P3} + \dot{Z}_{P3} = \dot{C}_6$	$\dot{B}_7 + \dot{B}_{W,P3} + \dot{Y}_{P3} = \dot{B}_6$	$c_{W,P3} = 0.5\frac{\$}{MJ}$, $b_{W,P3} = 7.5\frac{mPts}{MJ}$
Overall system	$\dot{C}_1 + \sum\dot{C}_W + \sum\dot{Z} = \dot{C}_3 + \dot{C}_Q$	$\dot{B}_1 + \sum\dot{B}_W + \sum\dot{Y} = \dot{B}_3 + \dot{B}_Q$	$c_W = 0.5\frac{\$}{MJ}$, $c_Q = 0.0511\frac{\$}{MJ}$ $b_W = 7.5\frac{mPts}{MJ}$ $b_Q = 5.4\frac{mPts}{MJ}$

where R is the thermal resistance for geothermal pipes (with a length of L) buried in the soil in terms of the fluid temperature (T_i) and soil temperature (T_o) [45]. Detailed information about all heat transfer phenomena can be found in Refs. [12,46].

The power need of the system is determined considering the pressure drops (ΔP) and required energy for the compression states (Δh). Assuming the efficiency (η) of 80 %, the required powers for the pumps and compressor are given by:

$$\dot{W}_P = \frac{\dot{m} v \Delta P}{\eta} \tag{32}$$

$$\dot{W}_{Comp} = \frac{\dot{m}((\Delta h) + (v(\Delta P_{Con-side} + \Delta P_{TES-side})))}{\eta} \tag{33}$$

3.4. Determination of the decision makers for GDHS

The exergetic outputs of any energy system are the critical parameters since the exergy defines the energy's quality and quantity. The exergy drives the efficient use of an energy source. So, the exergy efficiency (ε) was determined as the first decision maker. It is given by:

$$\varepsilon = 1 - \frac{\dot{E}x_d}{\dot{E}x_{in}} \tag{34}$$

where $\dot{E}x_d$ is the destructed exergy, and $\dot{E}x_{in}$ is the exergy given to any system or component. Depending on the efficient design of any energy system, the sustainability of an energy source can be determined in terms of exergy efficiency. Therefore, the sustainability index (SI) was selected as the second decision maker. SI is given by Ref. [47]:

$$SI = \frac{1}{1 - \varepsilon} \tag{35}$$

As well as exergetic indicators, economic and environmental issues are also crucial for any energy system. Therefore, the economic and environmental indicators related to exergy output are valuable parameters for analyzing energy systems. In this regard, the relative costs (r) and relative environmental impacts (r_b) were selected as the third and fourth decision makers, respectively. Since the EATWOS aims for the maximum output, the reverse of relative cost ($1/r_k$) and relative environmental impact ($1/r_{b,k}$) should be taken into account in calculations [46,48]:

$$\frac{1}{r} = \frac{c_F}{c_P - c_F} \tag{36}$$

$$\frac{1}{r_b} = \frac{b_F}{b_P - b_F} \tag{37}$$

where $c_{F,k}$ and $c_{P,k}$ are the unit cost of the exergy flows for the fuel and product, respectively. $b_{F,k}$ and $b_{P,k}$ are the specific environmental impact for the fuel and product, respectively [49]. The related values are obtained through the exergy, exergoeconomic and exergoenvironmental analyses mentioned in sections 3.1 and 3.2. The detailed information can be found in Ref. [46]. Although the relative cost produces valuable insight, it does not give enough information from the investment point of view. To deal with this indeterminacy, the net present value (NPV) was selected as the fifth decision maker. NPV is given by Ref. [50]:

$$NPV = \sum_{t=0}^{n} \frac{B}{(1+r)^t} - I \tag{38}$$

where B, r, n, I and t are the cash flow, the discount rate (15.75 %), the lifetime of the system (20 years), the investment cost and the related year, respectively.

4. Results and discussion

In the study, 37 essential cases were formed considering the different thermodynamic parameters and PCM for a single refrigerant. Later, these cases were expanded to 111 cases for three different refrigerants. The working fluids were selected, taking into consideration environmental issues such as the global warming potential (GWP) and ozone depletion potential (ODP). The thermodynamic behaviors of the refrigerants (such as wet, dry and isentropic types) were also considered. In this regard, R600a as the dry type, R290 as the wet type and R1234ze as the isentropic type were used in the analysis. In forming the cases, the available limits of the temperature differences for an effective heat transfer were considered. Also, the temperature scales as the determinative thermodynamic property were tried to be kept equivalent or closer as much as possible for a clear comparison. Since R290 enables flexibility in the temperature scale due to the wet-type state changing, the cases were expanded to 148 for a more comprehensive investigation. The formed cases and analysis results for the decision maker are given in Tables 6–9.

4.1. Results of ANN modeling

In this study, 15 input parameters were used to train the ANN for the estimating of 5 output parameters. In ANN modeling, T_1, T_2, T_3, T_4, T_5, T_6, T_7, T_8, T_9, T_a, T_b, T_c, and T_d in ^oC were used to define the system configurations. T_m in ^oC was used to define the selected PCM, whereas specific heat value (C_p) in kJ/kg was used to define the selected refrigerant. Output parameters were selected as SI, ε, 1/r, $1/r_b$ and NPV for the reasons mentioned in Section 3.4. The Levenberg-Marguardt (LM) algorithm was used as the training along with the linear transfer function (Purelin). Using MATLAB, 70% of the formed cases (randomly selected) were used for the ANN training, whereas the remaining part was used to test the ANN model. It is a need to observe the orientation of the ANN results without bias for embedding the ANN weights into EATWOS. So, the outputs with and without bias were also investigated. The results are given in Figs. 4–8.

In Fig. 4, the findings obtained for SI are given. The R^2 value of the training step was obtained as 0.9995, whereas it was determined as 0.9996 for the testing step. The overall R^2 value was obtained as 0.9995. In the case with bias, the polynomial trends of the formed cases for the analytic and ANN with bias results substantially overlap. So, the ANN model strongly agrees with the analytic outputs. In the case without bias, the tendency of the results is compatible with those of the analytic and ANN models. The R^2 value between the ANN results with bias and without bias was recorded as 1 in compliance with the nature of the Purelin function. This evidence clearly shows that the obtained weights for SI can be sensitively used in MCDM analysis.

In Fig. 5, the findings obtained for ε are given. The R^2 value of the training step was obtained as 0.9990, whereas it was determined as 0.9975 for the testing step. The overall R^2 value was obtained as 0.9984. In the case with bias, the polynomial trends of the formed cases for the analytic and ANN with bias results substantially overlap. So, the ANN model strongly agrees with the analytic outputs. In the case without bias, the tendency of the results is compatible with those of the analytic and ANN models. The R^2 value between the ANN results with bias and without bias was recorded as 1 in compliance with the nature of the Purelin function. This evidence clearly shows that the obtained weights for ε can be sensitively used in MCDM analysis.

In Fig. 6, the findings obtained for $1/r$ are given. The R^2 value of the training step was obtained as 0.9995, whereas it was determined as 0.9996 for the testing step. The overall R^2 value was obtained as 0.9995. In the case with bias, the polynomial trends of the formed cases for the analytic and ANN with bias results substantially overlap. So, the ANN model strongly agrees with the analytic outputs. In the case without bias, the tendency of the results is compatible with those of the analytic and ANN models. The R^2 value between the ANN results with bias and

Table 6
The formed cases and analysis results for R600a.

Cases	T_1	T_2	T_3	T_4	T_5	T_6	T_7	T_8	T_9	T_a	T_b	T_c	T_d	T_m	C_p	P_a	P_b	SI	ε	1/r	$1/r_b$	NPV
1	100	99.89	72.00	94.89	94.80	55	40	67	66.94	40	70.76	70	33	60	1.6923	440.01	1087.50	1.14	12.36	0.001330	0.000943	−1.32
2	100	99.89	71.73	94.89	94.80	55	40	66	65.94	45	73.81	70	35	60	1.6923	464.77	1087.50	1.15	12.93	0.001395	0.000965	−1.59
3	100	99.89	70.62	94.89	94.80	45	30	65	64.94	40	60.85	50	25	60	1.6923	350.67	684.90	1.09	7.98	0.000802	0.000546	−1.43
4	100	99.89	70.51	94.89	94.80	45	30	65	64.94	40	60.01	50	26	60	1.6923	361.02	684.90	1.09	8.02	0.000794	0.000546	−0.81
5	100	99.89	70.61	94.89	94.80	45	30	65	64.94	40	60.79	55	30	60	1.6923	404.72	772.99	1.09	7.98	0.000793	0.000545	−0.89
6	100	99.89	71.11	94.89	94.80	55	45	65	64.94	45	70.44	60	29	60	1.6923	393.45	869.16	1.17	14.74	0.001594	0.001091	−0.94
7	110	109.87	80.93	104.87	104.78	60	40	75	74.93	55	75.26	55	30	70	1.6923	404.72	772.99	1.18	14.91	0.001588	0.001223	0.91
8	110	109.87	81.46	104.87	104.78	60	40	75	74.93	55	79.20	60	30	70	1.6923	404.72	869.16	1.17	14.66	0.001577	0.001220	0.16
9	95	94.89	66.51	89.89	89.81	50	40	60	59.95	40	65.71	61	30	55	1.6923	404.72	889.40	1.14	12.46	0.001314	0.000921	−2.78
10	95	94.89	65.84	89.89	89.81	45	35	60	59.95	40	60.79	55	30	55	1.6923	404.72	772.99	1.11	9.73	0.000990	0.000688	−0.15
11	100	99.89	71.05	94.89	94.80	55	40	66	65.94	43	65.25	60	33	55	1.6923	440.01	869.16	1.16	13.47	0.001451	0.000994	2.97
12	100	99.89	70.02	94.89	94.80	55	40	65	64.95	50	66.39	60	40	60	1.6923	531.21	869.16	1.17	14.23	0.001536	0.000976	6.47
13	100	99.89	70.55	94.89	94.80	55	40	65	64.94	45	65.61	60	35	60	1.6923	464.77	869.16	1.16	13.96	0.001506	0.000989	2.83
14	100	99.89	70.83	94.89	94.80	55	40	65	64.94	45	65.59	55	30	55	1.6923	404.80	772.99	1.16	14.10	0.001515	0.001017	0.84
15	100	99.89	70.19	94.89	94.80	45	30	65	64.95	40	57.56	47	26	60	1.6923	361.02	635.74	1.09	8.11	0.000812	0.000545	0.69
16	100	99.89	70.04	94.89	94.80	45	30	65	64.95	50	66.49	47	27	60	1.6923	371.60	635.74	1.09	8.15	0.000819	0.000544	2.40
17	100	99.89	70.59	94.89	94.80	55	45	65	64.94	45	65.59	55	30	60	1.6923	404.72	772.99	1.18	15.15	0.001653	0.001096	1.31
18	100	99.89	70.70	94.89	94.80	55	45	65	64.94	45	66.41	55	29	60	1.6923	393.45	772.99	1.18	15.09	0.001647	0.001096	0.85
19	110	109.87	80.41	104.87	104.78	60	40	75	74.94	55	71.30	50	30	70	1.6923	404.72	684.90	1.18	15.19	0.001650	0.001229	6.29
20	110	109.87	80.40	104.87	104.78	60	40	75	74.94	55	71.20	60	40	70	1.6923	531.21	869.16	1.18	15.19	0.001654	0.001219	6.76
21	110	109.87	80.29	104.87	104.78	60	40	75	74.94	55	70.41	60	41	70	1.6923	545.30	869.16	1.18	15.24	0.001658	0.001217	7.22
22	110	109.87	80.30	104.87	104.78	60	40	75	74.94	55	70.41	54	35	70	1.6923	464.77	754.74	1.18	15.24	0.001661	0.001225	7.74
23	95	94.89	65.84	89.89	89.81	50	40	60	59.95	40	60.79	55	30	55	1.6923	404.72	772.99	1.15	12.79	0.001361	0.000924	0.46
24	95	94.89	65.08	89.89	89.81	45	35	60	59.95	40	55.05	48	30	55	1.6923	404.72	651.82	1.11	10.01	0.001026	0.000688	3.46
25	100	99.89	70.34	94.89	94.80	45	30	65	64.94	40	56.94	40	20	55	1.6923	302.22	531.21	1.09	8.23	0.000824	0.000562	0.92
26	100	99.89	70.02	94.89	94.80	60	50	65	64.95	50	66.39	60	40	60	1.6923	531.21	869.16	1.22	18.24	0.002049	0.001299	3.51
27	100	99.89	70.55	94.89	94.80	60	50	65	64.94	45	65.61	60	35	60	1.6923	464.77	869.16	1.22	17.90	0.002006	0.001314	−0.20
28	100	99.89	70.05	94.89	94.80	55	45	65	64.95	45	61.55	50	30	60	1.6923	404.72	684.90	1.18	15.41	0.001674	0.001093	3.54
29	110	109.87	80.40	104.87	104.78	65	55	75	74.94	55	71.20	60	40	70	1.6923	531.21	869.16	1.25	20.24	0.002326	0.001708	3.76
30	110	109.87	80.29	104.87	104.78	65	55	75	74.94	55	70.41	60	41	70	1.6923	545.30	869.16	1.25	20.30	0.002331	0.001704	4.08
31	110	109.87	80.30	104.87	104.78	65	45	75	74.94	55	70.41	54	35	70	1.6923	464.77	754.74	1.22	18.00	0.002006	0.001477	5.05
32	95	94.89	65.08	89.89	89.81	50	40	60	59.95	40	55.05	48	30	55	1.6923	404.72	651.82	1.15	13.04	0.001363	0.000915	0.04
33	95	94.89	65.08	89.89	89.81	50	35	60	59.95	40	55.05	48	30	55	1.6923	404.72	651.82	1.13	11.75	0.001209	0.000808	0.59
34	110	109.87	80.40	104.87	104.78	65	50	75	74.94	55	71.21	55	35	70	1.6923	464.77	772.99	1.24	19.19	0.002166	0.001600	3.38
35	100	99.89	70.05	94.89	94.80	55	40	65	64.95	45	61.55	50	30	60	1.6923	404.72	684.90	1.17	14.20	0.001523	0.000990	4.39
36	100	99.89	70.05	94.89	94.80	55	35	65	64.95	45	61.55	50	30	60	1.6923	404.72	684.90	1.15	12.79	0.001350	0.000880	4.21
37	110	109.87	80.40	104.87	104.78	65	45	75	74.94	55	71.21	55	35	70	1.6923	464.77	772.99	1.22	17.94	0.002003	0.001478	4.92

Table 7
The formed cases and analysis results for R290.

Cases	T_1	T_2	T_3	T_4	T_5	T_6	T_7	T_8	T_9	T_a	T_b	T_c	T_d	T_m	C_p	P_a	P_b	SI	ε	1/r	$1/r_b$	NPV
38	100	99.89	72.41	94.89	94.80	55	40	67	66.94	40	79.94	70	33	60	1.6847	1160.80	2586.80	1.14	12.22	0.001315	0.000933	−3.69
39	100	99.89	72.11	94.89	94.80	55	40	66	65.94	45	82.34	70	35	60	1.6847	1217.90	2586.80	1.15	12.77	0.001377	0.000951	−4.22
40	100	99.89	70.79	94.89	94.80	45	30	65	64.94	40	66.38	50	25	60	1.6847	952.07	1716.30	1.09	7.94	0.000799	0.000541	−2.26
41	100	99.89	70.67	94.89	94.80	45	30	65	64.94	40	65.30	50	26	60	1.6847	976.53	1713.30	1.09	7.97	0.000803	0.000540	−1.17
42	100	99.89	71.17	94.89	94.80	45	30	65	64.94	40	66.58	55	30	60	1.6847	1079.00	1907.20	1.08	7.82	0.000788	0.000537	−4.61
43	100	99.89	71.51	94.89	94.80	55	45	65	64.94	45	77.37	60	29	60	1.6847	1052.70	2116.80	1.17	14.69	0.001611	0.001084	−2.50
44	110	109.87	81.13	104.87	104.78	60	40	75	74.93	55	80.56	55	30	70	1.6847	1079.00	1907.20	1.17	14.82	0.001607	0.001209	0.89
45	110	109.87	81.73	104.87	104.78	60	40	75	74.93	55	85.64	60	30	70	1.6847	1079.00	2116.80	1.17	14.52	0.001583	0.001205	−1.20
46	95	94.89	66.77	89.89	89.81	50	40	60	59.95	40	72.97	61	30	55	1.6847	1079.00	2160.60	1.14	12.34	0.001317	0.000907	−4.24
47	95	94.89	66.02	89.89	89.81	45	35	60	59.95	40	66.58	55	30	55	1.6847	1079.00	1907.20	1.11	9.67	0.000997	0.000678	−1.15
48	100	99.89	71.28	94.89	94.80	55	40	66	65.94	43	71.71	60	33	55	1.6847	1160.80	2116.80	1.15	13.38	0.001443	0.000977	1.81
49	100	99.89	70.30	94.89	94.80	55	40	65	64.94	50	71.29	60	40	60	1.6847	1369.40	2116.80	1.16	14.10	0.001523	0.000953	4.99
50	100	99.89	70.80	94.89	94.80	55	40	65	64.94	45	71.59	60	35	60	1.6847	1217.90	2116.80	1.16	13.85	0.001496	0.000974	1.84
51	100	99.89	71.02	94.89	94.80	55	40	65	64.94	45	71.19	55	30	55	1.6847	1079.00	1907.20	1.16	14.01	0.001509	0.001000	0.45
52	100	99.89	70.32	94.89	94.80	45	30	65	64.94	40	62.16	47	26	60	1.6847	976.53	1604.20	1.09	8.07	0.000811	0.000540	0.43
53	100	99.89	70.18	94.89	94.80	45	30	65	64.95	50	70.68	47	27	60	1.6847	1001.40	1604.20	1.09	8.11	0.000816	0.000536	1.95
54	100	99.89	70.78	94.89	94.80	55	45	65	64.94	45	71.19	55	30	60	1.6847	1079.00	1907.20	1.18	15.07	0.001648	0.001083	1.04
55	100	99.89	70.89	94.89	94.80	55	45	65	64.94	45	72.17	55	29	60	1.6847	1052.70	1907.20	1.18	15.01	0.001642	0.001085	0.19
56	110	109.87	80.56	104.87	104.78	60	40	75	74.94	55	75.50	50	30	70	1.6847	1079.00	1713.30	1.18	15.12	0.001647	0.001213	5.91
57	110	109.87	80.58	104.87	104.78	60	40	75	74.94	55	75.91	60	40	70	1.6847	1369.40	2116.80	1.18	15.11	0.001652	0.001198	6.84
58	110	109.87	80.46	104.87	104.78	60	40	75	74.94	55	74.93	60	41	70	1.6847	1401.30	2116.80	1.18	15.17	0.001652	0.001195	6.59
59	110	109.87	80.44	104.87	104.78	60	40	75	74.94	55	74.61	54	35	70	1.6847	1217.90	1867.20	1.18	15.18	0.001657	0.001207	7.30
60	95	94.89	66.02	89.89	89.81	50	40	60	59.95	40	66.58	55	30	55	1.6847	1079.00	1907.20	1.15	12.71	0.001355	0.000911	0.00
61	95	94.89	65.20	89.89	89.81	45	35	60	59.95	40	59.15	48	30	55	1.6847	1079.00	1640.00	1.11	9.98	0.001025	0.000677	3.18
62	100	99.89	70.45	94.89	94.80	45	30	65	64.94	40	61.05	40	20	55	1.6847	836.46	1369.40	1.09	8.20	0.000823	0.000557	0.69
63	100	99.89	70.19	94.89	94.80	60	50	65	64.95	50	71.29	60	40	60	1.6847	1369.40	2116.80	1.22	18.17	0.002051	0.001270	3.82
64	100	99.89	70.80	94.89	94.80	60	50	65	64.94	45	71.59	60	35	60	1.6847	1217.90	2116.80	1.22	17.80	0.002005	0.001298	−0.29
65	100	99.89	70.19	94.89	94.80	55	45	65	64.95	45	65.97	50	30	60	1.6847	1079.00	1713.30	1.18	15.37	0.001678	0.001081	4.04
66	110	109.87	80.58	104.87	104.78	65	55	75	74.94	55	75.91	60	40	70	1.6847	1369.40	2116.80	1.25	20.17	0.002329	0.001680	4.00
67	110	109.87	80.46	104.87	104.78	65	55	75	74.94	55	74.93	60	41	70	1.6847	1401.30	2116.80	1.25	20.25	0.002337	0.001677	4.44
68	110	109.87	80.45	104.87	104.78	65	45	75	74.94	55	74.61	54	35	70	1.6847	1217.90	1867.20	1.22	17.93	0.002008	0.001457	5.49
69	95	94.89	65.20	89.89	89.81	50	40	60	59.95	40	59.15	48	30	55	1.6847	1079.00	1640.00	1.15	13.07	0.001376	0.000906	1.62
70	95	94.89	65.20	89.89	89.81	50	35	60	59.95	40	59.19	48	30	55	1.6847	1079.00	1640.00	1.13	11.73	0.001215	0.000797	1.83
71	110	109.87	80.56	104.87	104.78	65	50	75	74.94	55	75.64	55	35	70	1.6847	1217.90	1907.20	1.24	19.12	0.002170	0.001578	3.87
72	100	99.89	70.19	94.89	94.80	55	40	65	64.95	45	66.97	50	30	60	1.6847	1079.00	1713.30	1.16	14.16	0.001524	0.000978	4.28
73	100	99.89	70.19	94.89	94.80	55	35	65	64.95	45	65.97	50	30	60	1.6847	1079.00	1713.30	1.15	12.74	0.001349	0.000869	4.32
74	110	109.87	80.56	104.87	104.78	65	45	75	74.94	55	75.64	55	35	70	1.6847	1217.90	1907.20	1.22	17.86	0.002003	0.001457	5.01

Table 8
The formed cases and analysis results for R1234ze.

Cases	T_1	T_2	T_3	T_4	T_5	T_6	T_7	T_8	T_9	T_a	T_b	T_c	T_d	T_m	C_p	P_a	P_b	SI	ε	1/r	$1/r_b$	NPV
75	100	99.89	72.20	94.89	94.80	55	40	67	66.94	40	74.71	70	33	60	0.88733	630.75	1611.10	1.14	12.30	0.001308	0.000927	−2.43
76	100	99.89	71.91	94.89	94.80	55	40	66	65.94	45	77.50	70	35	60	0.88733	667.56	1611.10	1.15	12.86	0.001371	0.000942	−2.63
77	100	99.89	70.93	94.89	94.80	45	30	65	64.94	40	62.79	50	25	55	0.88733	498.59	997.45	1.09	8.06	0.000800	0.000548	−2.03
78	100	99.89	70.57	94.89	94.80	45	30	65	64.94	40	61.91	50	26	60	0.88733	513.85	997.45	1.09	8.00	0.000793	0.000535	−1.03
79	100	99.89	70.69	94.89	94.80	45	30	65	64.94	40	62.99	55	30	60	0.88733	578.43	1130.70	1.09	7.96	0.000792	0.000533	−1.24
80	100	99.89	71.36	94.89	94.80	55	45	65	64.94	45	73.16	60	29	60	0.88733	561.75	1276.80	1.17	14.76	0.001599	0.001074	−1.73
81	110	109.87	81.01	104.87	104.78	60	40	75	74.93	55	77.31	55	30	70	0.88733	578.43	1130.70	1.17	14.88	0.001588	0.001191	0.99
82	110	109.87	81.57	104.87	104.78	60	40	75	74.93	55	81.75	60	30	70	0.88733	578.43	1276.80	1.17	14.60	0.001572	0.001194	−0.34
83	95	94.89	66.63	89.89	89.81	50	40	60	59.95	40	68.58	61	30	55	0.88733	578.43	1307.70	1.14	12.41	0.001309	0.000899	−3.63
84	95	94.89	65.91	89.89	89.81	45	35	60	59.95	40	62.99	55	30	55	0.88733	578.43	1130.70	1.11	9.71	0.000987	0.000669	−0.53
85	100	99.89	71.16	94.89	94.80	55	40	66	65.94	43	67.86	60	33	55	0.88733	630.75	1276.80	1.16	13.43	0.001447	0.000960	2.36
86	100	99.89	70.09	94.89	94.80	55	40	65	64.95	50	68.41	60	40	60	0.88733	630.75	1276.80	1.17	14.20	0.001533	0.000923	5.95
87	100	99.89	70.68	94.89	94.80	55	40	65	64.94	45	68.01	60	35	60	0.88733	667.56	1276.80	1.16	13.91	0.001500	0.000958	2.06
88	100	99.89	70.91	94.89	94.80	55	40	65	64.94	45	65.59	55	30	55	0.88733	578.43	1130.70	1.16	14.07	0.001511	0.000982	0.24
89	100	99.89	70.24	94.89	94.80	45	30	65	64.94	40	59.18	47	26	60	0.88733	513.85	923.39	1.09	8.10	0.000812	0.000534	0.63
90	100	99.89	70.09	94.89	94.80	45	30	65	64.95	50	67.99	47	27	60	0.88733	529.46	923.39	1.09	8.14	0.000818	0.000529	2.22
91	100	99.89	70.67	94.89	94.80	55	45	65	64.94	45	67.72	55	30	60	0.88733	578.43	1130.70	1.18	15.13	0.001652	0.001068	1.16
92	100	99.89	70.78	94.89	94.80	55	45	65	64.94	45	68.60	55	29	60	0.88733	561.75	1130.70	1.18	15.06	0.001645	0.001071	0.61
93	110	109.87	80.47	104.87	104.78	60	40	75	74.94	55	72.86	50	30	70	0.88733	578.43	997.15	1.18	15.17	0.001649	0.001193	6.11
94	110	109.87	80.46	104.87	104.78	60	40	75	74.94	55	73.14	60	40	70	0.88733	766.63	1276.80	1.18	15.17	0.001658	0.001169	7.46
95	110	109.87	80.36	104.87	104.78	60	40	75	74.94	55	72.28	60	41	70	0.88733	787.70	1276.80	1.18	15.22	0.001656	0.001162	6.95
96	110	109.87	80.36	104.87	104.78	60	40	75	74.94	55	72.05	54	35	70	0.88733	667.56	1103.00	1.18	15.22	0.001659	0.001181	7.46
97	95	94.89	65.91	89.89	89.81	50	40	60	59.95	40	62.99	55	30	55	0.88733	578.43	1130.70	1.15	12.75	0.001359	0.000898	0.38
98	95	94.89	65.13	89.89	89.81	45	35	60	59.95	40	56.53	48	30	55	0.88733	578.43	947.60	1.11	10.00	0.001026	0.000664	3.32
99	100	99.89	70.38	94.89	94.80	45	30	65	64.94	40	58.27	40	20	55	0.88733	427.38	766.63	1.09	8.22	0.000824	0.000550	0.67
100	100	99.89	70.09	94.89	94.80	60	50	65	64.95	50	68.42	60	40	60	0.88733	766.30	1276.80	1.22	18.24	0.002052	0.001226	3.56
101	100	99.89	70.68	94.89	94.80	60	50	65	64.94	45	68.01	60	35	60	0.88733	667.56	1276.80	1.22	17.86	0.002006	0.001272	−0.19
102	100	99.89	70.11	94.89	94.80	55	45	65	64.95	45	63.17	50	30	60	0.88733	578.43	997.45	1.18	15.41	0.001677	0.001060	3.68
103	110	109.87	80.47	104.87	104.78	65	55	75	74.94	55	73.14	60	40	70	0.88733	766.63	1276.80	1.25	20.23	0.002330	0.001633	3.94
104	110	109.87	80.36	104.87	104.78	65	55	75	74.94	55	72.28	60	41	70	0.88733	787.70	1276.80	1.25	20.29	0.002336	0.001625	4.42
105	110	109.87	80.30	104.87	104.78	65	45	75	74.94	55	72.05	54	35	70	0.88733	667.56	1103.00	1.22	17.97	0.002007	0.001420	5.26
106	95	94.89	65.13	89.89	89.81	50	40	60	59.95	40	56.53	48	30	55	0.88733	578.43	947.60	1.15	13.07	0.001371	0.000881	0.78
107	95	94.89	65.13	89.89	89.81	50	35	60	59.95	40	55.05	48	30	55	0.88733	578.43	947.60	1.13	11.75	0.001209	0.000776	0.48
108	110	109.87	80.47	104.87	104.78	65	50	75	74.94	55	72.94	55	35	70	0.88733	667.56	1130.70	1.24	19.17	0.002170	0.001540	3.76
109	100	99.89	70.11	94.89	94.80	55	40	65	64.95	45	63.17	50	30	60	0.88733	578.43	997.45	1.17	14.19	0.001524	0.000961	4.62
110	100	99.89	70.11	94.89	94.80	55	35	65	64.95	45	63.17	50	30	60	0.88733	578.43	997.45	1.15	12.78	0.001350	0.000854	4.33
111	110	109.87	80.47	104.87	104.78	65	45	75	74.94	55	72.94	55	35	70	0.88733	667.56	1130.70	1.22	17.92	0.002004	0.001424	4.95

Table 9
The extended cases and analysis results for R290.

Cases	T_1	T_2	T_3	T_4	T_5	T_6	T_7	T_8	T_9	T_a	T_b	T_c	T_d	T_m	C_p	P_a	P_b	SI	ε	1/r	$1/r_b$	NPV
112	100	99.89	72.41	94.89	94.80	60	40	67	66.94	40	79.94	70	33	60	1.6847	1160.80	2586.80	1.16	13.53	0.001475	0.001041	−3.80
113	100	99.89	72.11	94.89	94.80	60	40	66	65.94	45	82.34	70	35	60	1.6847	1217.90	2586.80	1.16	14.13	0.001545	0.001062	−4.29
114	100	99.89	70.79	94.89	94.80	50	40	65	64.94	40	66.38	50	25	60	1.6847	952.07	1716.30	1.14	12.22	0.001294	0.000867	0.08
115	100	99.89	70.67	94.89	94.80	50	40	65	64.94	40	65.30	50	26	60	1.6847	976.53	1713.30	1.14	12.28	0.001300	0.000867	0.73
116	100	99.89	71.17	94.89	94.80	50	40	65	64.94	40	66.58	55	30	60	1.6847	1079.00	1907.20	1.14	12.06	0.001281	0.000862	−1.55
117	100	99.89	71.51	94.89	94.80	60	40	65	64.94	45	77.37	60	29	60	1.6847	1052.70	2116.80	1.18	14.93	0.001633	0.001093	−3.22
118	110	109.87	81.13	104.87	104.78	65	40	75	74.93	55	80.56	55	30	70	1.6847	1079.00	1907.20	1.19	16.22	0.001794	0.001338	2.38
119	110	109.87	81.73	104.87	104.78	60	40	75	74.93	55	85.64	60	30	70	1.6847	1079.00	2116.80	1.17	14.52	0.001583	0.001205	−1.20
120	95	94.89	66.77	89.89	89.81	55	40	60	59.95	40	72.97	61	30	55	1.6847	1079.00	2160.60	1.16	13.97	0.001513	0.001032	−3.87
121	95	94.89	66.02	89.89	89.81	50	40	60	59.95	40	66.58	55	30	55	1.6847	1079.00	1907.20	1.15	12.71	0.001355	0.000911	0.00
122	100	99.89	71.28	94.89	94.80	55	45	66	65.94	43	71.71	60	33	55	1.6847	1160.80	2116.80	1.17	14.56	0.001596	0.001080	2.00
123	100	99.89	70.30	94.89	94.80	55	45	65	64.94	50	71.29	60	40	60	1.6847	1369.40	2116.80	1.18	15.34	0.001686	0.001055	5.12
124	100	99.89	70.80	94.89	94.80	55	45	65	64.94	45	71.59	60	35	60	1.6847	1217.90	2116.80	1.18	15.07	0.001655	0.001078	2.02
125	100	99.89	71.02	94.89	94.80	55	45	65	64.94	45	71.19	55	30	55	1.6847	1079.00	1907.20	1.18	15.23	0.001668	0.001106	0.50
126	100	99.89	70.32	94.89	94.80	45	35	65	64.94	40	62.16	47	26	60	1.6847	976.53	1604.20	1.10	9.46	0.000970	0.000646	2.17
127	100	99.89	70.18	94.89	94.80	45	35	65	64.95	50	70.68	47	27	60	1.6847	1001.40	1604.20	1.11	9.51	0.000977	0.000641	3.64
128	100	99.89	70.78	94.89	94.80	60	40	65	64.94	45	71.19	55	30	60	1.6847	1079.00	1907.20	1.18	15.35	0.001680	0.001094	1.46
129	100	99.89	70.89	94.89	94.80	60	40	65	64.94	45	72.17	55	29	60	1.6847	1052.70	1907.20	1.18	15.28	0.001674	0.001096	1.12
130	110	109.87	80.56	104.87	104.78	65	40	75	74.94	55	75.50	50	30	70	1.6847	1079.00	1713.30	1.20	16.54	0.001821	0.001340	4.66
131	110	109.87	80.58	104.87	104.78	65	40	75	74.94	55	75.91	60	40	70	1.6847	1369.40	2116.80	1.20	16.52	0.001829	0.001323	5.95
132	110	109.87	80.46	104.87	104.78	60	45	75	74.94	55	74.93	60	41	70	1.6847	1401.30	2116.80	1.20	16.48	0.001826	0.001316	6.73
133	110	109.87	80.44	104.87	104.78	65	40	75	74.94	55	74.61	54	35	70	1.6847	1217.90	1867.20	1.20	16.60	0.001832	0.001332	6.08
134	95	94.89	66.02	89.89	89.81	55	45	60	59.95	40	66.58	55	30	55	1.6847	1079.00	1907.20	1.19	15.64	0.001714	0.001145	−1.06
135	95	94.89	65.20	89.89	89.81	45	30	60	59.95	40	59.15	48	30	55	1.6847	1079.00	1640.00	1.09	8.52	0.000856	0.000566	1.50
136	100	99.89	70.45	94.89	94.80	50	30	65	64.94	40	61.05	40	20	55	1.6847	836.46	1369.40	1.11	9.82	0.000999	0.000672	0.74
137	100	99.89	70.19	94.89	94.80	60	40	65	64.95	50	71.29	60	40	60	1.6847	1369.40	2116.80	1.19	15.67	0.001714	0.001063	4.84
138	100	99.89	70.80	94.89	94.80	60	40	65	64.94	45	71.59	60	35	60	1.6847	1217.90	2116.80	1.18	15.32	0.001672	0.001086	0.26
139	100	99.89	70.19	94.89	94.80	60	40	65	64.95	45	65.97	50	30	60	1.6847	1079.00	1713.30	1.19	15.67	0.001703	0.001090	3.17
140	110	109.87	80.58	104.87	104.78	70	40	75	74.94	55	75.91	60	40	70	1.6847	1369.40	2116.80	1.22	17.90	0.002003	0.001448	4.51
141	110	109.87	80.46	104.87	104.78	70	40	75	74.94	55	74.93	60	41	70	1.6847	1401.30	2116.80	1.22	17.97	0.002009	0.001444	4.95
142	110	109.87	80.45	104.87	104.78	70	40	75	74.94	55	74.61	54	35	70	1.6847	1217.90	1867.20	1.22	17.98	0.002002	0.001457	4.07
143	95	94.89	65.20	89.89	89.81	55	35	60	59.95	40	59.15	48	30	55	1.6847	1079.00	1640.00	1.15	13.38	0.001410	0.000917	2.49
144	95	94.89	65.20	89.89	89.81	55	30	60	59.95	40	59.15	48	30	55	1.6847	1079.00	1640.00	1.13	11.83	0.001223	0.000800	1.33
145	110	109.87	80.56	104.87	104.78	70	40	75	74.94	55	75.64	55	35	70	1.6847	1217.90	1907.20	1.22	17.91	0.002000	0.001458	3.62
146	100	99.89	70.19	94.89	94.80	60	35	65	64.95	45	66.97	50	30	60	1.6847	1079.00	1713.30	1.17	14.25	0.001527	0.000980	3.06
147	100	99.89	70.19	94.89	94.80	60	35	65	64.95	45	65.97	50	30	60	1.6847	1079.00	1713.30	1.17	14.25	0.001526	0.000980	3.29
148	110	109.87	80.56	104.87	104.78	70	40	75	74.94	55	75.64	55	35	70	1.6847	1217.90	1907.20	1.22	17.91	0.001999	0.001458	3.89

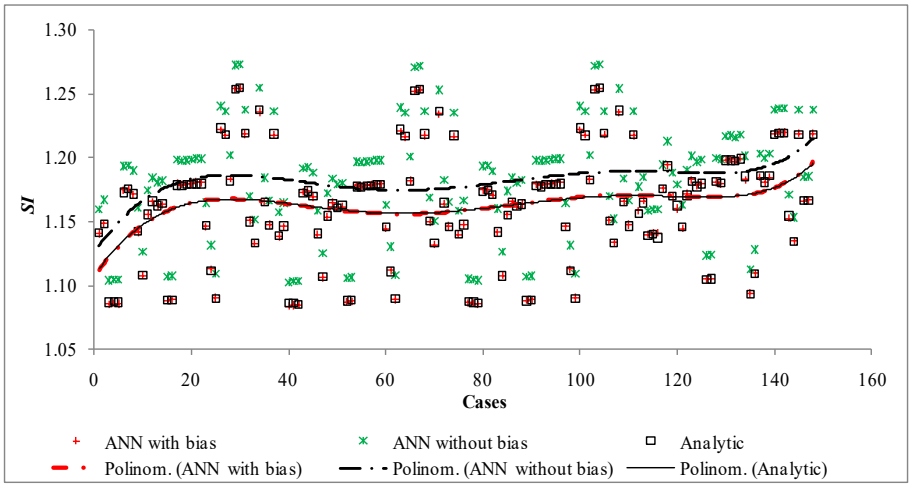

Fig. 4. ANN results for SI.

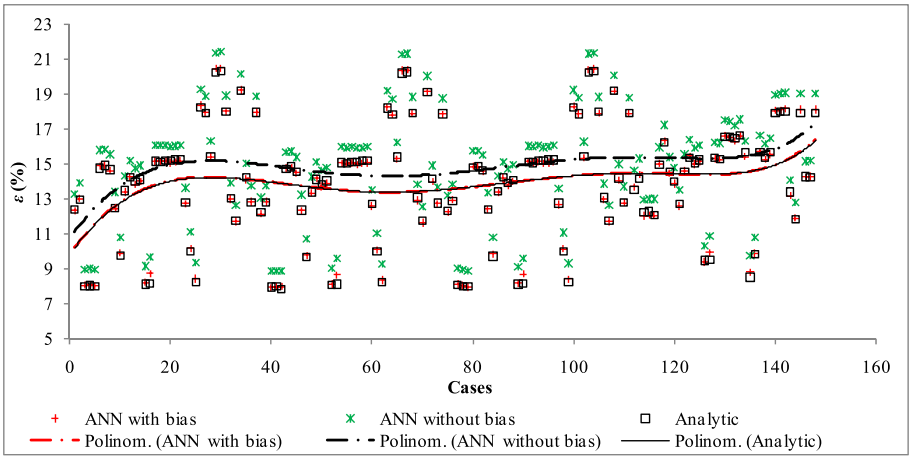

Fig. 5. ANN results for ε.

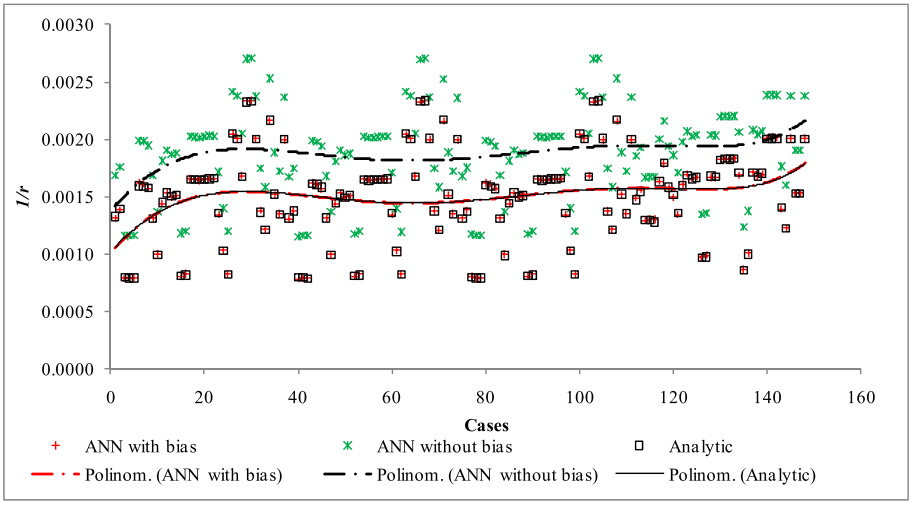

Fig. 6. ANN results for *1/r*.

without bias was recorded as 1 in compliance with the nature of the Purelin function. This evidence clearly shows that the obtained weights for *1/r* can be sensitively used in MCDM analysis.

In Fig. 7, the findings obtained for $1/r_b$ are given. The R^2 value of the training step was obtained as 0.9970, whereas it was determined as 0.9980 for the testing step. The overall R^2 value was obtained as 0.9973. In the case with bias, the polynomial trends of the formed cases for the analytic and ANN with bias results substantially overlap. So, the ANN

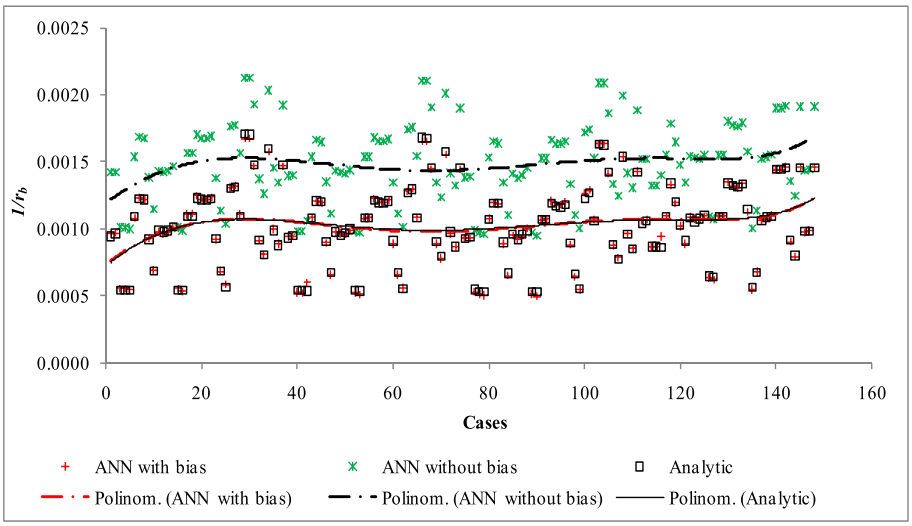

Fig. 7. ANN results for $1/r_b$.

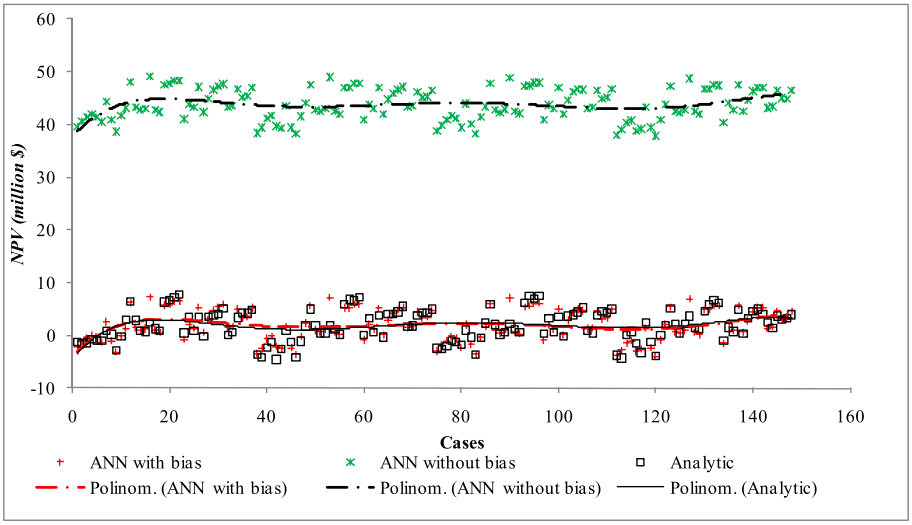

Fig. 8. ANN results for NPV.

model strongly agrees with the analytic outputs. In the case without bias, the tendency of the results is compatible with those of the analytic and ANN models. The R^2 value between the ANN results with bias and without bias was recorded as 1 in compliance with the nature of the Purelin function. This evidence clearly shows that the obtained weights for $1/r_b$ can be sensitively used in MCDM analysis.

In Fig. 8, the findings obtained for *NPV* are given. The R^2 value of the training step was obtained as 0.9046, whereas it was determined as 0.7385 for the testing step. The overall R^2 value was obtained as 0.8451. In the case with bias, the polynomial trends of the formed cases for the analytic and ANN with bias results substantially overlap. So, the ANN model strongly agrees with the analytic outputs. In the case without bias, the tendency of the results is compatible with those of the analytic and ANN models. The R^2 value between the ANN results with bias and without bias was recorded as 1 in compliance with the nature of the Purelin function. This evidence clearly shows that the obtained weights for *NPV* can be sensitively used in MCDM analysis. According to these findings, the weights of the input parameters for each output are obtained as follows:

$$\mathbf{W}_{\mathrm{ANN}} = \begin{bmatrix} & \boldsymbol{SI} & \boldsymbol{\varepsilon} & \boldsymbol{1/r} & \boldsymbol{1/r_b} & \boldsymbol{NPV} \\ \boldsymbol{T_1} & 0.165425 & 0.029475 & 0.144544 & 0.005611 & 0.087411 \\ \boldsymbol{T_2} & 0.164663 & 0.028856 & 0.144106 & 0.005302 & 0.087376 \\ \boldsymbol{T_3} & 0.002291 & 0.001747 & 0.001683 & 0.003444 & 0.001004 \\ \boldsymbol{T_4} & 0.165046 & 0.029121 & 0.144331 & 0.005410 & 0.087386 \\ \boldsymbol{T_5} & 0.495894 & 0.087530 & 0.433654 & 0.014380 & 0.262335 \\ \boldsymbol{T_6} & 0.001497 & 0.001068 & 0.000854 & 0.000364 & 0.000009 \\ \boldsymbol{T_7} & 0.001314 & 0.000886 & 0.000779 & 0.000325 & 0.000007 \\ \boldsymbol{T_8} & 0.002918 & 0.411226 & 0.065886 & 0.482697 & 0.237670 \\ \boldsymbol{T_9} & 0.000098 & 0.409468 & 0.063766 & 0.481587 & 0.236715 \\ \boldsymbol{T_a} & 0.000074 & 0.000163 & 0.000030 & 0.000107 & 0.000038 \\ \boldsymbol{T_b} & 0.000166 & 0.000126 & 0.000026 & 0.000239 & 0.000012 \\ \boldsymbol{T_c} & 0.000334 & 0.000201 & 0.000167 & 0.000274 & 0.000015 \\ \boldsymbol{T_d} & 0.000246 & 0.000114 & 0.000135 & 0.000161 & 0.000012 \\ \boldsymbol{T_m} & 0.000029 & 0.000020 & 0.000040 & 0.000080 & 0.000010 \\ \boldsymbol{C_p} & 0.000005 & 0.000001 & 0.000000 & 0.000018 & 0.000001 \end{bmatrix} \tag{39}$$

4.2. Results of AHP analysis

In the determination of the AHP weights for the ranking of the output parameters, the comparison matrix is offered according to the expert

views:

$$\mathbf{A}=\begin{bmatrix} & \boldsymbol{SI} & \boldsymbol{\varepsilon} & \mathbf{1}/\boldsymbol{r} & \mathbf{1}/\boldsymbol{r_b} & \boldsymbol{NPV} \\ \boldsymbol{SI} & 1 & 1 & 2 & 2 & 0.33 \\ \boldsymbol{\varepsilon} & 1 & 1 & 0.5 & 0.33 & 0.25 \\ \mathbf{1}/\boldsymbol{r} & 0.5 & 2 & 1 & 0.5 & 0.5 \\ \mathbf{1}/\boldsymbol{r_b} & 0.5 & 3 & 2 & 1 & 0.5 \\ \boldsymbol{NPV} & 3 & 4 & 2 & 2 & 1 \end{bmatrix} \quad (40)$$

The significance matrix is then obtained as follows:

$$\mathbf{B}=\begin{bmatrix} & \boldsymbol{SI} & \boldsymbol{\varepsilon} & \mathbf{1}/\boldsymbol{r} & \mathbf{1}/\boldsymbol{r_b} & \boldsymbol{NPV} \\ \boldsymbol{SI} & 0.1667 & 0.0909 & 0.2667 & 0.3429 & 0.1290 \\ \boldsymbol{\varepsilon} & 0.1667 & 0.0909 & 0.0667 & 0.0571 & 0.0968 \\ \mathbf{1}/\boldsymbol{r} & 0.0833 & 0.1818 & 0.1333 & 0.0857 & 0.1935 \\ \mathbf{1}/\boldsymbol{r_b} & 0.0833 & 0.2727 & 0.2667 & 0.1714 & 0.1935 \\ \boldsymbol{NPV} & 0.5000 & 0.3636 & 0.2667 & 0.3429 & 0.3871 \end{bmatrix} \quad (41)$$

in the light of the significance matrix, the ranking matrix which produces the weights of the output parameters is obtained as:

$$\mathbf{W}_{\mathrm{AHP}}=\begin{bmatrix} \boldsymbol{SI} & 0.199226 \\ \boldsymbol{\varepsilon} & 0.095632 \\ \mathbf{1}/\boldsymbol{r} & 0.135550 \\ \mathbf{1}/\boldsymbol{r_b} & 0.197541 \\ \boldsymbol{NPV} & 0.372051 \end{bmatrix} \quad (42)$$

The randomized indicator (*RI*) is taken as 1.12 for the analysis with 5 outputs according to the literature data [16]. So, the consistency of the determined weights (*CR*) is obtained as 0.082. Since *CR* is lower than the value of 0.1, the obtained weight scores are acceptable for the MCDM analysis.

4.3. Results of the ANN-AHP-EATWOS hybrid model

Using the weights of ANN and AHP, the hybrid MCDM model was conducted for 15 input and 5 output parameters. The designed GDHS system was optimized through MCDM for all input parameters. The obtained results for the efficiency of GDHS are given in Fig. 9.

Fig. 9. Results of the hybrid ANN-AHP-EATWOS tool for all output parameters.

In Fig. 9, it is seen that the efficiencies range between 0.8976 and 0.9734. According to MCDM results, Case 67 was determined as the most effective case. In this case, the design parameters of T_1, T_2, T_3, T_4, T_5, T_6, T_7, T_8, T_9, T_a, T_b, T_c, and T_d were conducted as 110 °C, 109.87 °C, 80.46 °C, 104.87 °C, 104.78 °C, 65 °C, 55 °C, 75 °C, 74.94 °C, 55 °C, 74.93 °C, 60 °C, and 41 °C, respectively. The evaporator (P_a) and condenser (P_b) pressures were conducted as 1401.3 kPa and 2116.8 kPa, respectively. The most efficient fluid was conducted as R290, whereas the most efficient PCM was conducted as RT70HC with a melting temperature of 70 °C. In this case, the exergy efficiency was calculated as 20.25 %, whereas the SI was determined as 1.25, with the highest score. $1/r$ and $1/r_b$ were determined as 0.002337 and 0.001677, respectively. The NPV value was determined as 4.44 million $.

The analysis was also conducted in the study for each single output parameter. The handled analysis in this way can also be defined as ANN-EATWOS analysis since there is no AHP weight for the output scores. The obtained results are given in Figs. 10–14.

According to Fig. 10, the most efficient case was determined as case 134. In this case, the exergy efficiency was calculated as 15.64 %, whereas the SI was determined as 1.19 with the highest score. $1/r$ and $1/r_b$ were determined as 0.001714 and 0.001145, respectively. The NPV value was determined as −1.06 million $. As can be seen from these results, the conducted design is not profitable for the investment.

According to Fig. 11, the most efficient case was determined as case 30. In this case, the exergy efficiency was calculated as 20.30 %, whereas the SI was determined as 1.25, with the highest score. $1/r$ and $1/r_b$ were determined as 0.002331 and 0.001704, respectively. The NPV value was determined as 4.08 million $. Although the design is profitable and has higher exergy efficiency with lower exergoenvironmental impact, the relative exergoeconomic cost is higher.

According to Fig. 12, the most efficient case was also determined as case 67 in the manner of ANN-AHP-EATWOS results. This obtaining shows that the exergoeconomic factor is the main collimating factor.

According to Fig. 13, the most efficient case was determined as case 29. In this case, the exergy efficiency was calculated as 20.24 %, whereas the SI was determined as 1.25 with the highest score. $1/r$ and $1/r_b$ were

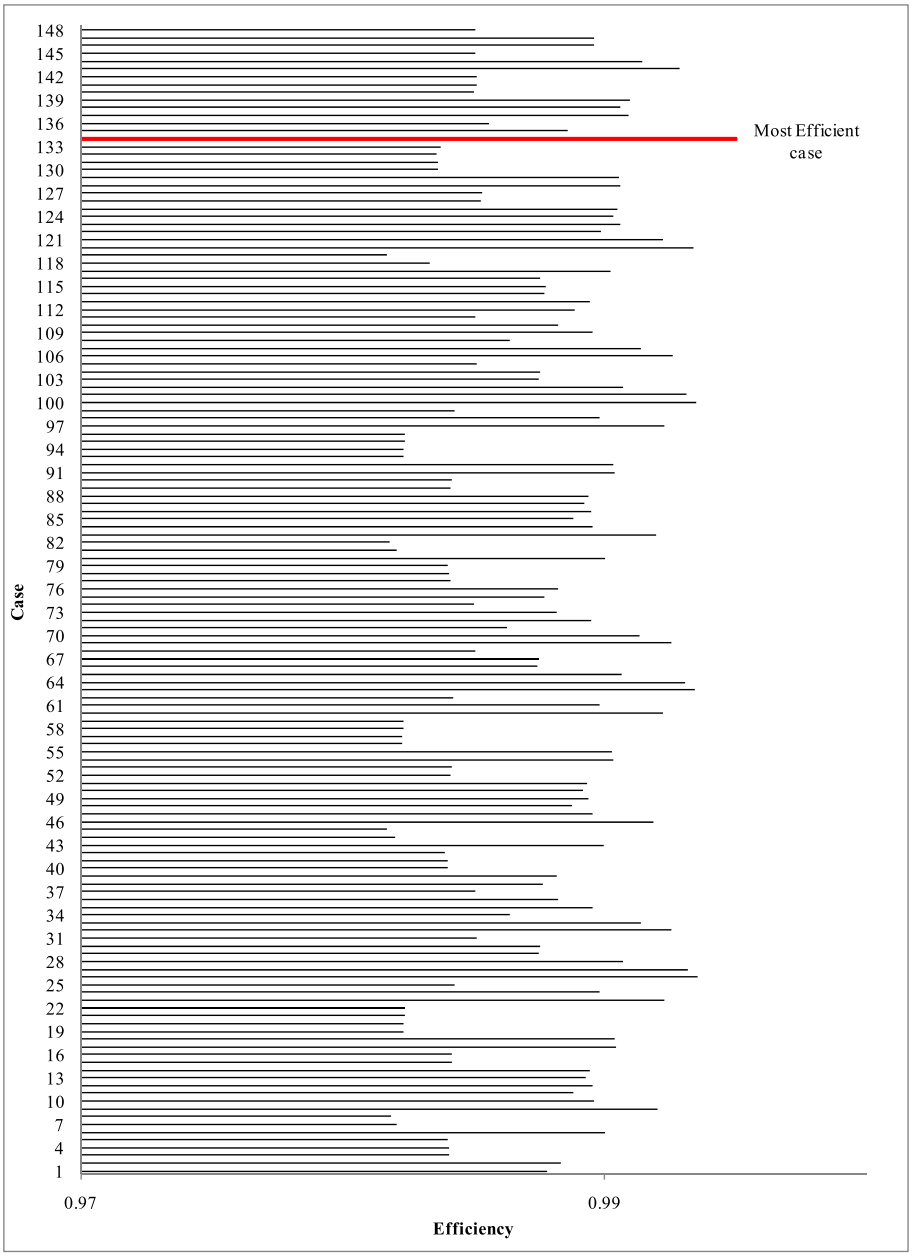

Fig. 10. Results of the ANN-EATWOS hybrid tool for SI.

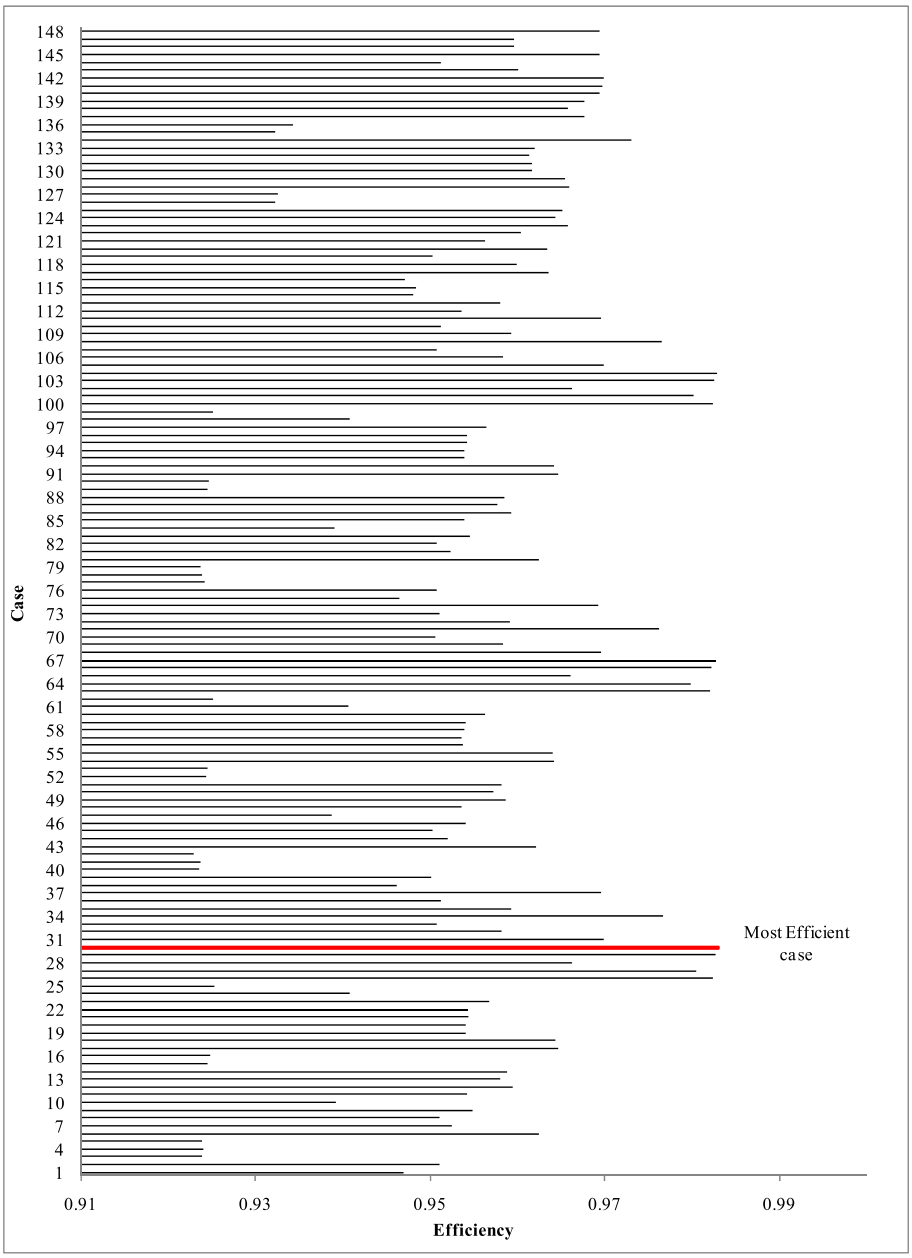

Fig. 11. Results of the ANN-EATWOS hybrid tool for ε.

determined as 0.002326 and 0.001708, respectively. The NPV value was determined as 3.76 million $. Although the design is profitable and has closer values to those of ANN-AHP-EATWOS results, the relative exergoeconomic cost is higher.

According to Fig. 14, the most efficient case was determined as case 22. In this case, the exergy efficiency was calculated as 15.24 %, whereas the SI was determined as 1.18 with the highest score. $1/r$ and $1/r_b$ were determined as 0.001661 and 0.001225, respectively. The NPV value was determined as 7.74 million $. Although the design is the most profitable one, the relative exergoeconomic cost and exergoenvironmental impact are higher. Besides, the exergy efficiency is lower, and neither is the SI.

4.4. Final decision on the optimal GDHS

ANN-AHP-EATWOS results show that the weightings of the design (input) parameters are critical, as well as the weightings of the decision parameters when compared to analysis with a single output. So, all the output parameters should be evaluated simultaneously to make a sensible decision for a sustainable, exergy-efficient, environment-friendly, and profitable design. In this study, the optimal design was determined as the case 67. The technical characteristics, energy and exergy analysis results, exergoenvironmental analysis results, exergoeconomic analysis, and NPV results are given in Tables 10–14, respectively.

According to analyses, the exergy efficiency of the overall system was determined as 20.25 % with exergy destruction of 23,219.40 kW. The primary source of the exergy destruction was determined as the DTL and S. The relative cost (r) was determined as 427.95 %, whereas the exergoenvironmental impact (r_b) was determined as 596.27 %. The primary source of exergoenvironmental impact and the relative cost was determined as S system including the TES-driven HP. The NPV was obtained as 4,440,248.68 $, which means an investable system. The system's payback period was determined as approximately 5 years with a total investment cost of 24,774,330.84 $. The obtained results by the hybrid model for the handled system were compared with those of the classical weighted MCDM given by Ref. [46]. The conventional system was also

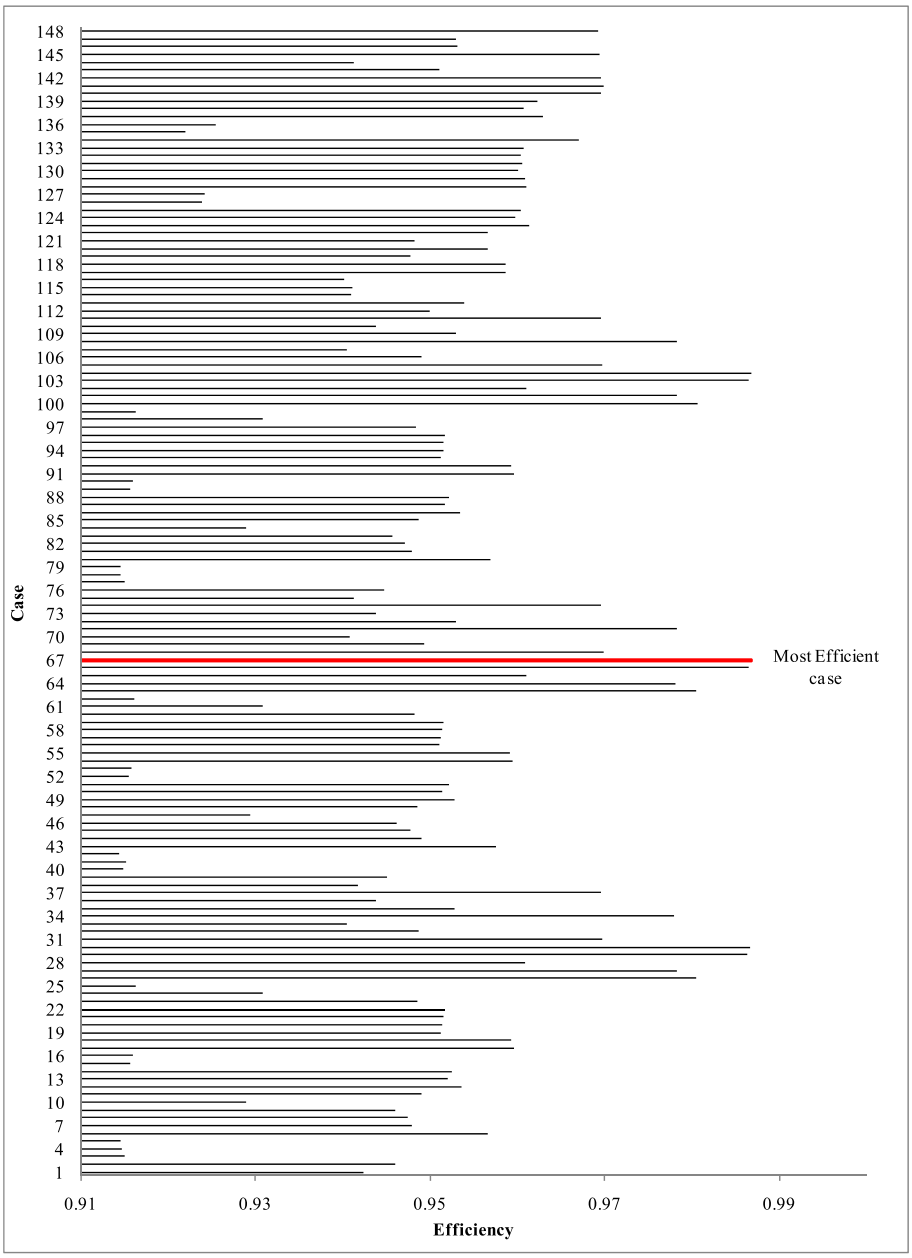

Fig. 12. Results of the ANN-EATWOS hybrid tool for 1/r.

analyzed for the same working conditions for the comparative evaluation. The comparative results are given in Table 15.

5. Conclusions

This study proposed a new hybrid multi-decision decision-making (MCDM). Artificial neural network (ANN) modeling was conducted first to determine the effects of input (design) parameters on the outputs. An analytic hierarchic process (AHP) was conducted later to determine the importance level of the outputs throughout the expert views. Finally, ANN and AHP were integrated into the efficiency analysis technique with output satisficing (EATWOS) for making a decision on the optimal solution. The proposed system was run for a geothermal district heating system (GDHS) including a subsystem with a TES-driven HP system. In this aim, 148 designs were formed considering thermodynamically limited values of the 15 different design parameters for 3 different refrigerants. The following findings were concluded:

- The proposed hybrid MCDM analysis technique is a handy tool due to more sensitive results since it cares about the impact levels of the input parameters and the importance level of the output parameters. The ANN tool successfully determines the impact levels (weightings) of the multiple design (input) parameters of energy systems. The AHP analysis successfully conducts the importance level of the multiple decision makers (outputs) through the expert views figured out according to the kind of energy system.
- The most potent input parameter of the designing stage of GDHS for the sustainability (*SI*) and relative cost ($1/r$) was determined as the inlet temperature of S (T_5). Also, the inlet temperature of GDHS (T_1) has an important impact on the designs from the viewpoint of *SI* and $1/r$. From the exergetic efficiency (ε) viewpoint, the most potent input parameter was determined as the outlet temperature of S (T_8) as well as the inlet temperature of S (T_5).
- According to the exergy-related economic and environmental evaluations, the most potent input parameter for the relative cost ($1/r$) was determined as the inlet temperature of S (T_5) as well as the inlet

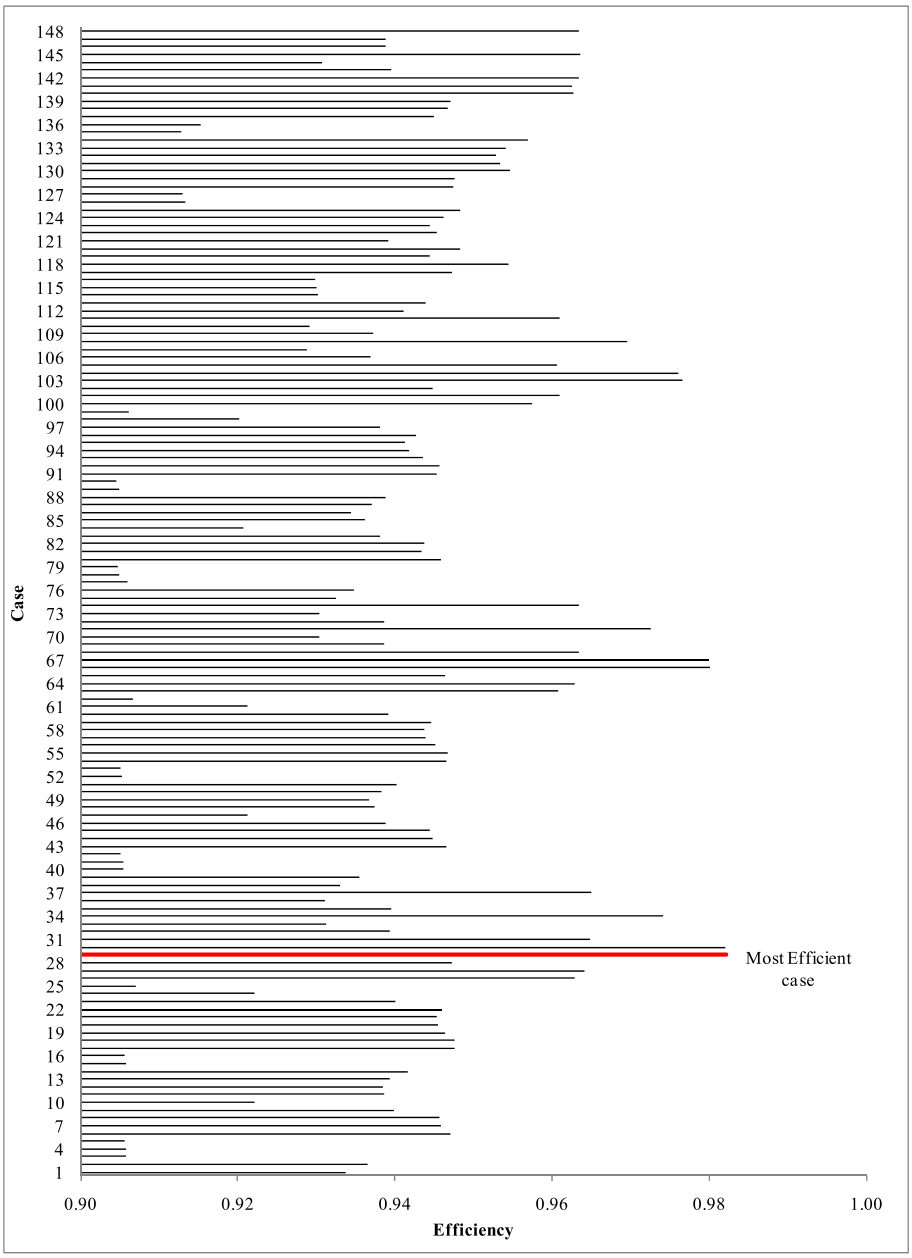

Fig. 13. Results of the ANN-EATWOS hybrid tool for $1/r_b$.

temperature of GDHS (T_1). For the relative environmental impact ($1/r_b$), the most potent input was determined as the inlet (T_5) and outlet (T_8) temperatures of S.

- From the economic evaluation side (*NPV*), the most potent input parameters were determined as the inlet temperature of S (T_5), the outlet temperature of S (T_8), and the inlet temperature of GDHS (T_1). Taking all the decision makers of the GDHS into account, the most potent input parameters can be defined as the inlet temperature of GDHS (T_1), the inlet temperature of S (T_5), and the outlet temperature of S (T_8), which guide the designing of the system.
- The most available working fluid was determined as the wet type refrigerant (R290) with a PCM with higher melting temperature depending on its thermodynamic behavior of refrigerant in larger temperature limits under the handled circumstances. The most efficient design was obtained for the higher inlet temperature of GDHS (T_1) by 110 °C and the outlet temperature of S (T_8) by 75 °C. However, the designs were conducted assuming a GDHS after a power cycle. So, the power generation issue should be evaluated in an integrated system to observe its impacts on the GDHS.

Credit author statement

Aslı Ergenekon Arslan: Data curation, Methodolgy, Investigation, Writing. **Oguz Arslan**: Analysis, Conceptualization, Methodology, Validation, Writing- Reviewing and Editing, Investigation. **M. Serdar Genc**: Analysis, Methodology, Validation.

Declaration of competing interest

The authors declare that they have no known competing financial interests or personal relationships that could have appeared to influence the work reported in this paper.

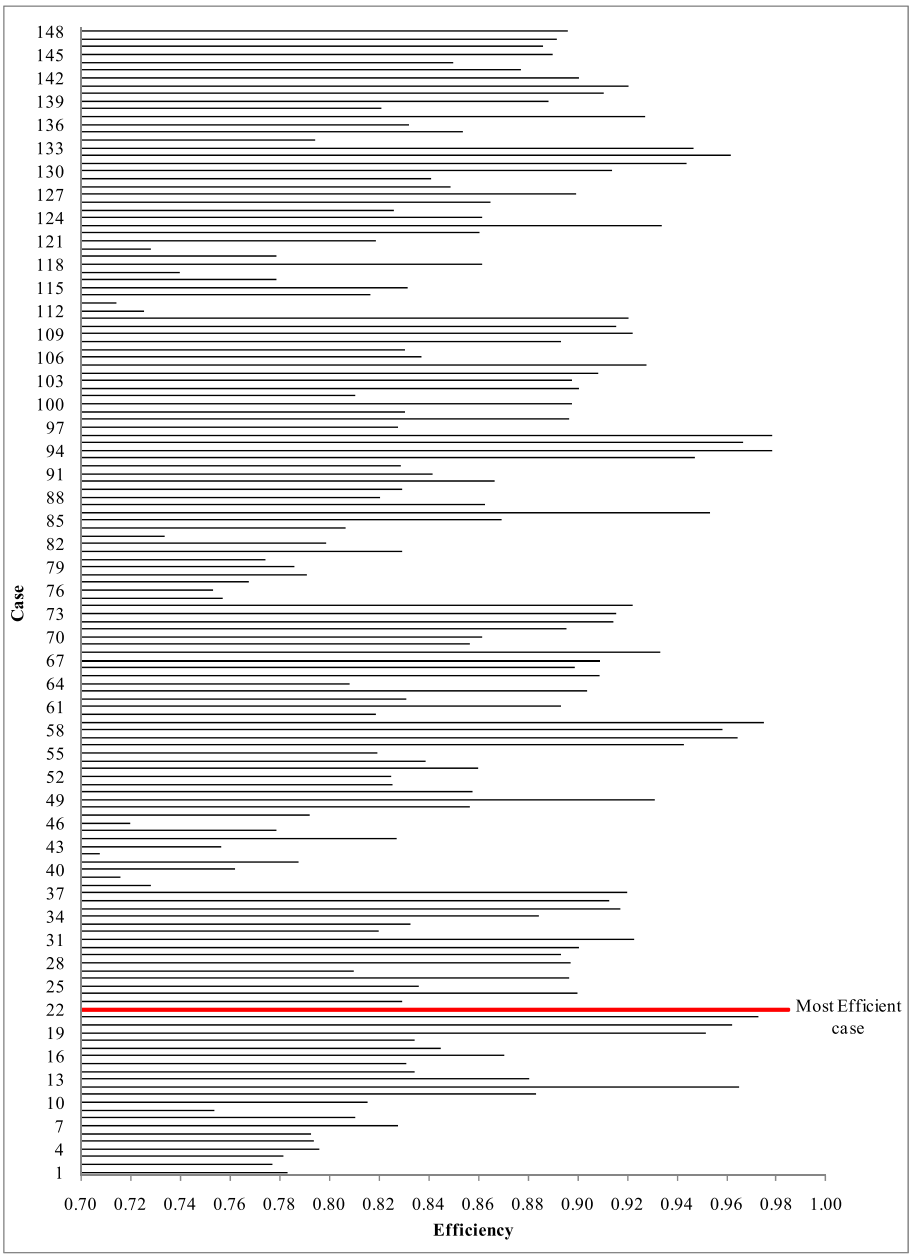

Fig. 14. Results of the ANN-EATWOS hybrid tool for NPV.

Table 10
Thermophysical characteristics of optimal GDHS.

Points	Fluids	$\dot{m}$ (kg/s)	T (°C)	P (kPa)	h (kJ/kg)	s (kJ/kg K)	v (m^3/kg)	ψ (kJ/kg)	$\dot{E}$ (kW)	$\dot{E}x$ (kW)
0	H_2O	–	25.00	101.33	104.82	0.3674	–	–	–	–
	R290				630.33	2.8445				
1	Geofluid	462.00	110.00		461.42	1.4188	0.001052	43.12	213,178.30	19,920.26
2	Geofluid	462.00	109.87		460.89	1.4174	0.001051	43.00	212,931.30	19,865.15
3	Geofluid	462.00	80.46		336.26	1.0792	0.001029	19.20	155,353.70	8872.19
4	H_2O	445.4339	104.87		439.75	1.3619	0.001047	38.39	196,949.46	17,194.47
5	H_2O	445.43	104.78		439.36	1.3609	0.001047	38.31	196,776.57	17,157.72
6	H_2O	1341.09	65.00		251.19	0.8313	0.001017	8.04	168,556.68	5398.42
7	H_2O	1341.09	55.00		167.54	0.5723	0.001008	1.62	112,426.68	1084.52
8	H_2O	445.43	75.00		314.03	1.0158	0.001026	15.86	140,644.27	7104.49
9	H_2O	445.43	74.94		313.76	1.0151	0.001026	15.82	140,523.42	7087.13
a	R290	191.96	55.00	1401.30	646.15	2.4361	0.035582	137.58	124034.32	26410.58
b	R290	191.96	74.93	2116.80	666.55	2.4361	0.023103	157.98	127950.29	30326.54
c	R290	191.96	60.00	2116.80	368.18	1.5426	0.002334	126.00	70674.78	24187.04
d	R290	191.96	41.00	1401.30	368.18	1.5529	0.007776	122.92	70674.78	23596.19

Table 11
Energy and exergy analysis results of optimal GDHS.

Components	$\dot{W}$ (kW)	$\dot{Q}$ (kW)	$\dot{E}_i$ (kW)	$\dot{E}_o$ (kW)	$\dot{E}x_f$ (kW)	$\dot{E}x_p$ (kW)	$\dot{E}x_d$ (kW)	η (%)	ε (%)
GTL	1535.00	−1781.99	213178.30	212931.30	21455.44	19865.15	1590.29	99.17	92.59
C		−1145.72	57285.92	56140.20	10943.87	10052.43	891.44	98.00	91.85
DTL	11035.72	−11329.47	335879.88	335586.13	35190.38	24112.62	11077.76	96.74	68.52
S	4902.93	−4619.38	55846.45	56130.00	14926.27	5870.89	9055.38	[a]11.65	39.33
HC	70.81	−56200.81	131048.11	74918.11	6501.42	5896.89	604.53	98.89	90.70
Overall system	***17544.4555***	***−18947.37***	***57532.91***	***56130.00***	***29116.29***	***5896.89***	***23219.40***	***74.22***	***20.25***

[a] COP value.

Table 12
Exergoenvironmental analysis results of optimal GDHS.

Components	Ý K (mPts/s)	bf.k (mPts/MJ)	$b_{p.k}$ (mPts/MJ)	$B_{d.k}$ (mPts/s)	$B_{total.k}$ (mPt/s)	f_b (%)	r_b (%)
GTL	4.91	1.30	1.65	2070.57	2075.48	0.2365	26.98
C	0.24	0.83	0.92	736.90	737.13	0.0321	11.71
DTL	8.03	3.48	5.41	38507.86	38515.90	0.0209	55.53
S	45.72	9.18	31.11	83085.95	83131.67	0.0550	239.12
HC	0.54	4.81	5.40	2910.38	2910.92	0.0187	12.17
Overall system	***59.44***	***4.98***	***34.66***	***115574.67***	***115634.11***	***0.0514***	***596.27***

Table 13
Exergoeconomic analysis results of optimal GDHS.

Components	ZK ($/s)	$c_{f.k}$ ($/MJ)	$c_{p.k}$ ($/MJ)	$\dot{c}_{d.k}$ ($/h)	$\dot{c}_{total.k}$ ($/h)	f (%)	r (%)
GTL	0.00868	0.07	0.08	415.35	415.36	0.0021	8.61
C	0.00839	0.04	0.04	126.43	126.44	0.0066	10.99
DTL	0.01643	0.23	0.34	9349.91	9349.93	0.0002	46.23
S	0.54391	0.57	1.55	18698.00	18698.54	0.0029	170.39
HC	0.05507	0.29	0.33	623.24	623.30	0.0088	13.51
Overall system	***0.63247***	***0.31***	***1.66***	***26222.14***	***26222.78***	***0.0024***	***427.95***

Table 14
NPV analysis results of optimal GDHS (in US$).

	Years					
	Present	1	5	10	15	20
Investment						
TES cost	−12,545,244.16					
Panel radiator addition cost	0.00					
Paraffin	−123,030.52					
Comp	−2,391,351.16					
Con	−9,389,705.00					
EV	−325,000.00					
Total	−24,774,330.84					
Cash flow						
Expenses						
Operating & Maintenance		62,726.22	62,726.22	62,726.22	62,726.22	62,726.22
Electricity benefit		2,504,138.31	2,504,138.31	2,504,138.31	2,504,138.31	2,504,138.31
Heat benefit		2,008,428.05	2,008,428.05	2,008,428.05	2,008,428.05	2,008,428.05
Salvage	2,477,433.08					
Total cash flow	−22,296,897.76	4,449,840.14	4,449,840.14	4,449,840.14	4,449,840.14	4,449,840.14
Cumulative cash flow	−22,296,897.76	−17,847,057.62	−47,697.06	22,201,503.63	44,450,704.33	66,699,905.02
Discount rate (15,75 %)	1.000	0.864	0.481	0.232	0.111	0.054
Present value	−22,296,897.76	3,908,077.44	2,177,103.93	1,047,789.79	504,277.00	242,696.86
NPV	**4,440,248.68**					

Table 15
The comparison of the optimal system.

Parameters	Present study	Ref. [46]	Conventional system
Fluid	R290	R1324ze	H_2O
ε (%)	20.25	19.17	12.45
SI	1.25	1.24	1.14
r (%)	427.95	460.85	709.80
rb (%)	596.27	649.50	755.70
NPV ($)	4,440,248.68	3,760,229.15	1,895,161.79

Data availability

No data was used for the research described in the article.

Nomenclature

A	area (m^2)
b	specific environmental impact (mPts/MJ)
$\dot{B}$	stream-related environmental impact (mPts/s)

c	unit cost of exergy flow ($/MJ)
$\dot{C}$	exergy cost rate ($/h)
CI	consistency indicator
CR	consistency of the determined weights
C_p	Specific heat (kJ/kg K)
D	diameter (m)
E	multicriteria efficiency
$\dot{E}$	energy rate (kW)
$\dot{Ex}$	exergy rate (kW)
f	exergoeconomic factor (%)
f_b	exergoenvironmental factor (%)
F	enforced convection boiling factor or correction factor
h	convective heat transfer coefficient (W/m^2K) or specific enthalpy (kJ/kg)
ip	distance matrices for input (kg/m^2s)
$\dot{m}$	mass flow rate (kg/s)
n	number of plates or pipes
op	distance matrices for output
P	pressure (kPa, bar or atm)
R	Thermal resistance
RI	Random indicator
$\dot{Q}$	heat rate (kW)
r	relative cost (%) or normalized output
r_b	relative environmental impact (%)
SI	sustainability index
T	temperature (K or ^oC)
U	Total heat transfer coefficient (W/m^2K)
v	weight for output
V	volume (m^3)
w	weight for input
$\dot{W}$	work rate (kW)
x	input value
y	output value
$\dot{Y}$	component-related environmental impact
$\dot{Z}$	investment cost

Greek symbols

β	volumetric expansion coefficient (−)
δ	weightings of ANN
ε	exergy efficiency (%)
η	Energy efficiency
λ	friction factor
μ	dynamic viscosity (Ns/m^2)
ν	specific volume (m^3/kg)
ρ	density (kg/m^3)

Subscripts

d	destruction
i	inner, inlet, or ith component
k	kth component
lm	logarithmic mean
m	melting
o	outer, outlet
0	value at the reference state

Superscripts

*	normalized values

Abbreviations

AHP	Analytic hierarchic process
ANN	Artificial neural network
C	Heat centre
Con	Condenser
Comp	Compressor
DTL	District transmission line

EV	Extension valve
GDHS	Geothermal district heating system
GTL	Geothermal transmission line
GWP	Global warming potential
HC	Heating circuit
HEx	Heat exchanger
HP	Heat pump
MCDM	Multicriteria decision making
NPV	Net present value
ODP	Ozone depletion potential
PCM	Phase change material
Rad	Panel radiator
S	Substation
TES	Thermal energy storage

References

[1] Lund JW, Toth AN. Direct utilization of geothermal energy 2020 worldwide review. Geothermics 2021;90:101915.
[2] Lund JW, Huttrer GW, Toth AN. Characteristics and trends in geothermal development and use, 1995 to 2020. Geothermics 2022;105:102522.
[3] Arslan O, Arslan AE. Pareto principle-based advanced exergetic evaluation of geothermal district heating system: Simav case study. J Build Eng 2022;58:105035.
[4] Roy D. Performance evaluation of a novel biomass-based hybrid energy system employing optimization and multi-criteria decision-making techniques. Sustain Energy Technol Assessments 2020;42:100861.
[5] Toopshekan A, Rahdan P, Rad MAV, Yousefi H, Astaraei FR. Evaluation of a standalone CHP-Hybrid system using a multi-criteria decision making due to the sustainable development goals. Sustain Cities Soc 2022;87:104170.
[6] Li S, Zhang L, Wang X, Zhu C. A decision-making and planning optimization framework for multi-regional rural hybrid renewable energy system. Energy Convers Manag 2022;273:116402.
[7] Han Z, Li X, Sun J, Wang M, Liu G. An interactive multi-criteria decision-making method for building performance design. Energy Build 2023;282:112793.
[8] Ridha HM, Gomes C, Hizam H, Ahmadipour M, Heidari AA, Chen H. Multi-objective optimization and multi-criteria decision-making methods for optimal design of standalone photovoltaic system: a comprehensive review. Renew Sustain Energy Rev 2021;135:110202.
[9] Li X, Chen J, Sun X, Zhao Y, Chong C, Dai Y, Wang CH. Multi-criteria decision making of biomass gasification-based cogeneration systems with heat storage and solid dehumidification of desiccant coated heat exchangers. Energy 2021;233:121122.
[10] Hai T, Delgarm N, Wang D, Karimi MH. Energy, economic, and environmental (3 E) examinations of the indirect-expansion solar heat pump water heater system: a simulation-oriented performance optimization and multi-objective decision-making. J Build Eng 2022;60:105068.
[11] Arslan O, Arslan AE. Performance evaluation and multi-criteria decision analysis of thermal energy storage integrated geothermal district heating system. Process Saf Environ Protect 2022;167:21–33.
[12] Arslan O, Arslan AE, Boukelia TE. Modelling and optimization of domestic thermal energy storage based heat pump system for geothermal district heating. Energy Build 2023:112792. 282.
[13] Zhao H, Li B, Lu H, Wang X, Li H, Guo S, Xue W, Wang Y. Economy-environment-energy performance evaluation of CCHP microgrid system: a hybrid multi-criteria decision-making method. Energy 2022;240:122830.
[14] Bac U, Alaloosi KAMS, Turhan C. A comprehensive evaluation of the most suitable HVAC system for an industrial building by using a hybrid building energy simulation and multi criteria decision making framework. J Build Eng 2021;37:102153.
[15] Manirambona E, Talai SM, imutai SK. Sustainability evaluation of power generation technologies using Multicriteria Decision Making: the Kenyan case. Energy Rep 2022;8:14901–14.
[16] Arslan AE, Arslan O, Kandemir SY. AHP–TOPSIS hybrid decision-making analysis: Simav integrated system case study. J Therm Anal Calorim 2021;145:1191–202.
[17] Usman M, Jonas D, Frey G. A methodology for multi-criteria assessment of renewable integrated energy supply options and alternative HVAC systems in a household. Energy Build 2022;273:112397.
[18] Yang X, Zheng X, Zhou Z, Miao H, Liu H, Wang Y, Zhang H, You S, Wei S. A novel multilevel decision-making evaluation approach for the renewable energy heating systems: a case study in China. J Clean Prod 2023;390:135934.
[19] Oner O, Khalilpour K. Evaluation of green hydrogen carriers: a multi-criteria decision analysis tool. Renew Sustain Energy Rev 2022;168:112764.
[20] Abdel-Basset M, Gamal A, Elkomy OM. Hybrid Multi-criteria Decision Making approach for the evaluation of sustainable photovoltaic farms locations. J Clean Prod 2021;328:129526.
[21] Abdel-Basset M, Gamal A, Chakrabortty RK, Ryan M. Development of a hybrid multi-criteria decision-making approach for sustainability evaluation of bioenergy production technologies: a case study. J Clean Prod 2021;290:125805.
[22] Saraswat SK, Digalwar AK. Evaluation of energy alternatives for sustainable development of energy sector in India: an integrated Shannon's entropy fuzzy multi-criteria decision approach. Renew Energy 2021;171:58–74.
[23] Elkadeem MR, Younes A, Sharshir SW, Campana PE, Wang S. Sustainable siting and design optimization of hybrid renewable energy system: a geospatial multi-criteria analysis. Appl Energy 2021;295:117071.
[24] Arslan O. Power generation from medium temperature geothermal resources: ANN-based optimization of Kalina cycle system-34. Energy 2011;36:2528–34.
[25] Arslan O. ANN-based determination of optimum working conditions of residential combustors with respect to optimum insulation. Energy Sources, Part A Recovery, Util Environ Eff 2014;36:2603–12.
[26] Tugcu A, Arslan O. Optimization of geothermal energy aided absorption refrigeration system—gaars: a novel ANN-based approach. Geothermics 2017;65:210–21.
[27] Arat H, Arslan O. Optimization of district heating system aided by geothermal heat pump: a novel multistage with multilevel ANN modelling. Appl Therm Eng 2017;111:608–23.
[28] Boukelia TE, Arslan O, Mecibah MS. ANN-based optimization of a parabolic trough solar thermal power plant. Appl Therm Eng 2016;107:1210–8.
[29] Arslan O, Yetik O. ANN based optimization of supercritical ORC-Binary geothermal power plant: Simav case study. Appl Therm Eng 2011;31:3922–8.
[30] Myers JH, Alpert MI. Determinant buying attributes: meaning and measurement. Marketing 1968;32(10):13–20.
[31] Saaty TL. Decision making with the analytic hierarchy process. Int J Serv Sci 2008;1(1):83–98.
[32] Saaty TL. Multi-criteria decision making: the analytic hierarchy process. second ed. Pittsburgh: RWS Publications; 1990.
[33] Peters ML, Zelewski S. Efficiency analysis under consideration of satisficing levels for output quantities. In Proceedings of the 17th annual conference of the production and operations management society (POMS) , April 28-May 01, 2006, Boston, USA.
[34] REFPROP. Reference. Fluid thermodynamics and transport properties. NIST reference database. Version 9.0. USA: National Institute of Standards and Technology, NIST; 2010.
[35] RUBITHERM. Phase change materials. Available from: https://www.rubitherm.eu/en/productcategory/organische-pcm-rt. Last access: October 23rd, 2023.
[36] Devotta S, Padalkar AS, Sane NK. Performance assessment of HC-290 as a drop-in substitute to HCFC-22 in a window air conditioner. Int J Refrigeration 2005;28:594–604.
[37] Saleh B. Parametric and working fluid analysis of a combined organic Rankine vapor compression refrigeration system activated by low-grade thermal energy. J Adv Res 2016;7:651–60.
[38] Meyer L, Tsatsaronis G, Buchgeister J, Schebek L. Exergoenvironmental analysis for evaluation of the environmental impact of energy conversion systems. Energy 2009;34:75–89.
[39] Bejan A, Tsatsaronis G, Moran MJ. Thermal design and optimization. New York: John Wiley and Sons; 1996.
[40] Eco-indicator 99. Manuel for designers; 2000. Available from: https://pre-sustainability.com/legacy/download/EI99_Manual.pdf.
[41] Demirdokum. PKKP 600 type panel radiator 2022. https://www.cimri.com/radyator/en-ucuz-demirdokum-pkkp-600-1000-panel-plus-radyator-fiyatlari,503553.
[42] Genceli OF. Heat exchangers. Istanbul: Birsen Publication; 1999 [in Turkish)].
[43] Jiangyin M&C Heat Parts. NT250L type heat exchangers 2022. https://turkish.heat-exchangergasket.com/sale-14362173-titanium-0-5mm-nt250l-plate-heat-exchanger-plate-for-sea-water-fluid.html.
[44] Kakac S, Liu H, Pramuanjaroenkij A. Heat exchangers selection, rating and thermal design. third ed. Florida: CRC Press, Taylor and Francis Group; 2012.
[45] Arslan O, Kose R. Exergoeconomic optimization of integrated geothermal system in Simav. Kutahya. Energy Conversion and Management 2010;51:663–76.
[46] Arslan O, Arslan AE, Kurtbas I. Exergoeconomic and exergoenvironmental based multi-criteria optimization of a new geothermal district heating system integrated with thermal energy storage driven heat pump. J Build Eng 2023;73:106733.

[47] Lu F, Zhu Y, Pan M, Li C, Yin J, Huang F. Thermodynamic, economic, and environmental analysis of new combined power and space cooling system for waste heat recovery in waste-to-energy plant. Energy Convers Manag 2020;226:113511.
[48] Mousavi AS, Mehrpooya M. A comprehensive exergy-based evaluation on cascade absorption-compression refrigeration system for low temperature applications-exergy, exergoeconomic, and exergoenvironmental assessments. J Clean Prod 2020;246:119005.
[49] Bejan A, Tsatsaronis G, Moran MJ. Thermal design and optimization. New York: John Wiley and Sons; 1996.
[50] Akbulut A, Oguz Arslan O, Arat H, Erbas O. Important aspects for the planning of biogas energy plants: malatya case study. Case Stud Therm Eng 2021;26:101076.